

Supporting Information for

Design and Study of Structural, Linear and Nonlinear Optical Properties of Chiral $[\text{Fe}(\text{phen})_3]^{2+}$ Complexes

Ahmad Naim,^a Yacine Bouhadja,^b Miguel Cortijo,^{a,c} Elen Duverger-Nédellec,^a Howard D. Flack,^{d†} Eric Freysz,^{e} Philippe Guionneau,^a Antonio Iazzolino,^e Amine Ould Hamouda,^e Patrick Rosa^{a*}, Olaf Stefańczyk,^a Ángela Valentín-Pérez^{a,c} and Mehdi Zeggar,^{a,b}*

^a CNRS, Univ. Bordeaux, ICMCB, UMR 5026, F-33600 Pessac, France. ^b Department of Chemistry, University of Annaba, BP 12-23200 Sidi-Ammar, Algérie. ^c CNRS, Univ. Bordeaux, CRPP, UMR 5031, F-33600 Pessac, France. ^d Chimie minérale, analytique et appliquée, Sciences II, Université de Genève, 30, quai Ernest-Ansermet CH-1211 Geneva Switzerland. ^e LOMA, UMR CNRS 5798, 351 Cours de la Libération, 33405 Talence Cedex, France.

Contents

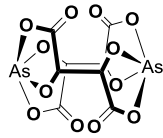
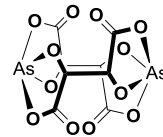
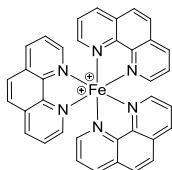
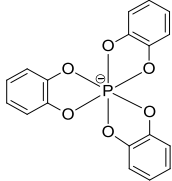
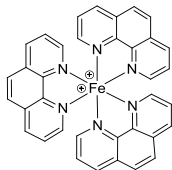
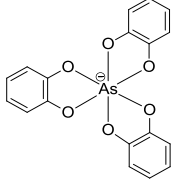
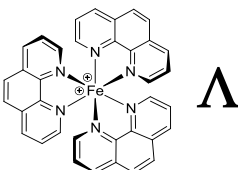
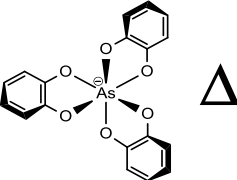
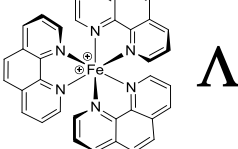
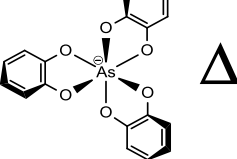
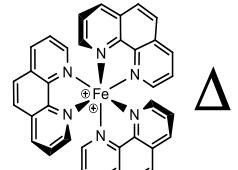
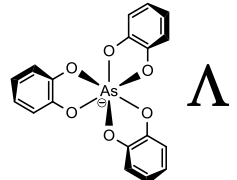
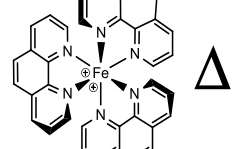
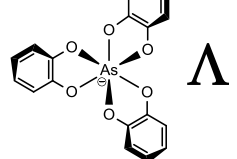
Table of compounds	5
General comments	6
X-ray powder diffraction and single crystal data collection and refinement	6
Salts of chiral anions	8
Synthesis	8
Crystallographic data for 1.....	11
Infrared data	14
Complexes	16
Synthesis of complexes 2-5	16
Crystallographic data for complexes 2-5	18
Synthesis of complexes 6-9	28
Crystallographic data for complexes 6-9	31
Spectroscopic data	36
Experimental details of CD and polarimeter measurements.....	36
Specific optical rotations of chiral anions.....	37
Absorption and CD spectra of $K_2[Sb_2(tartrate)_2]$ in water.....	38
Absorption and CD spectra of 1 in acetonitrile	39
CD spectra of 1 and $(NBu_4)_2(tartrate)$ in water.....	40
Solid state CD spectra of 1.....	41
Electronic spectra of complexes	42
Electronic and dichroic spectra of TRISCAS and alkaloid salts in acetonitrile	46
NMR spectra	47
CD spectra $[Fe(phen)_3](\Delta-TRISCAS)_2$ (4) recrystallized in acetonitrile.....	52
Second-harmonic generation measurements.....	53

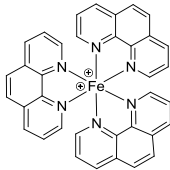
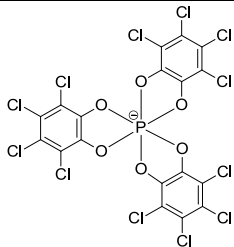
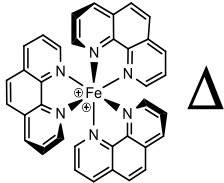
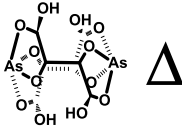
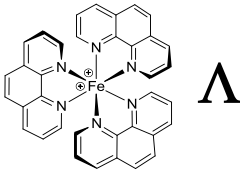
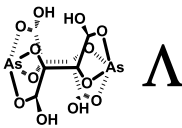
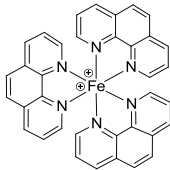
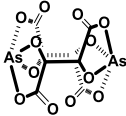
Table of Figures

Scheme S1. Synthesis of lipophilic racemic- tris(o-phenylenedioxy)arsenate(V) (TRISCAS) tetrabutylammonium.....	8
Figure S2. Asymmetric unit of Δ - 1 at 120 K.....	11
Table S3. Crystallographic data for $(\text{NBu}_4)_2[\text{As}_2(\text{tartrate})_2]\cdot 4\text{H}_2\text{O}$, Δ - 1 , Λ - 1 and rac- 1	12
Figure S4. Hydrogen bonding between butyl chains and oxygen atoms of hydroxyles/carboxyles of the anion and water molecules for 1	13
Figure S5. FTIR spectra of $(\text{NBu}_4)_2[\Lambda\text{-As}_2(\text{tartrate})_2]$ (blue line) Λ - 1 and $(\text{NBu}_4)_2[\Delta\text{-As}_2(\text{tartrate})_2]$ (red line) Δ - 1 in the solid state (top) and in solution in THF (bottom).....	14
Table S6. Point group analysis for complex 4	18
Figure S7. Plots of $(A_{\text{model}}, A_{\text{obs}})$, 2AD and Flack parameter determination from $(D_{\text{single}}, D_{\text{obs}})$ for complex 3	21
Figure S8. Plots of $(A_{\text{model}}, A_{\text{obs}})$, 2AD and Flack parameter determination from $(D_{\text{single}}, D_{\text{obs}})$ for complex 4	22
Table S9. Crystallographic data for complexes 2-5	23
Table S10. Average distances and interactions (\AA) for complexes 2-5	24
Figure S11. (top) Lateral interactions between Δ -TRISCAS and Λ -Fe(II) complexes in 3 . (bottom) Formation of Δ TRISCAS anionic shell around the triad structure in complex 3 as seen along the crystallographic <i>c</i> axis.....	25
Figure S12. Powder diffractograms of complexes 3 , 4 and 5 and corresponding powder diffraction patterns calculated from the X-ray structure.....	26
Table S13. Crystallographic data for complexes 4b , 5b , 4c , 5c	27
Table S14. Crystallographic data for complex 6	31
Table S15. Crystallographic data for complexes 7-9	32
Figure S16. Van der Waals representation of homochiral interactions in complexes 7 and 8 between $[\text{Fe}(\text{phen})_3]^{2+}$ and $[\text{As}_2(\text{tartrate})_2]^{2-}$	33
Figure S17. Crystal packing of complex 7 as seen along the <i>a</i> crystallographic axis. Cationic layers of $[\Lambda\text{-Fe}(\text{phen})_3]^{2+}$ are represented in red, counteranions are embedded within the positively charged layers shown in black.....	34
Figure S18. Comparison between bulk powder diffraction patterns (experimental) and calculated powder diffractograms for 7-9	35
Figure S19. Electronic absorption (top) and CD (bottom) spectra of $\text{K}_2[\Delta\text{-Sb}_2(\text{tartrate})_2]$ (red line) and $\text{K}_2[\Lambda\text{-Sb}_2(\text{tartrate})_2]$ (blue line) in water between 190-265 nm.....	38
Figure S20. Electronic absorption (top) and CD (bottom) spectra of Δ - 1 (red line) and Λ - 1 (blue line) in MeCN between 190-265 nm.....	39
Figure S21. Comparison of UV-Vis and CD spectra of 1 and $(\text{NBu}_4)_2(\text{tartrate})$ in water between 190-265 nm.....	40
Figure S22. CD spectra of KBr pellets of Δ - 1 (red line) and Λ - 1 (blue line) between 200-350 nm.....	41
Figure S23. UV-vis spectra of 2 (magenta line), 3 (black line), 4 (blue line), 5 (green line), $\text{NBu}_4(\text{rac-TRISCAS})$ (red line) measured in acetonitrile at room temperature. Solutions of complexes 2 and 3 were concentrated (saturation below 350 nm).....	42
Figure S25. Electronic absorption spectra of complexes 7 (black line), 8 (blue line), 9 (red line) measured in acetonitrile at room temperature.....	44
Table S26. Molar extinction coefficients for $[\text{Fe}(\text{phen})_3](\text{X})_2$, $\text{X} = \Delta$ - (7), Λ -arsenyl tartrate (8) and racemic mixture (9), measured in acetonitrile.....	45

Figure S27. (a top) CD spectra of (Δ -TRISCAS)cinchoninium and (Λ -TRISCAS)cinchonidinium in acetonitrile solution; (a bottom) electronic spectra of (Δ -TRISCAS)cinchoninium, (Λ -TRISCAS)cinchonidinium, cinchoninium and cinchonidinium CF_3COO^- salts, and TRISCAS(NBu_4) in acetonitrile solution; (b) CD spectra of cinchoninium and cinchonidinium CF_3COO^- salts in acetonitrile solution.....	46
Figure S28a. NMR spectra of $[\text{Fe}(\text{phen})_3](\text{rac-TRISCAS})_2$ (3) in d_3 -acetonitrile	47
Figure S28b. NMR spectra of $[\text{Fe}(\text{phen})_3](\text{rac-TRISCAS})_2$ (3) in d_6 -acetone.....	48
Figure S28c. NMR spectra of $[\text{Fe}(\text{phen})_3](\Delta\text{-TRISCAS})_2$ (4) in d_3 -acetonitrile	49
Figure S28d. NMR spectra of $[\text{Fe}(\text{phen})_3](\Delta\text{-TRISCAS})_2$ (4) in d_6 -acetone.....	50
Figure S29. CD spectra of KBr pellets with 4a recrystallized from acetonitrile.....	52
Figure S30. Complex $[\text{Fe}(\text{phen})_3](\Delta\text{-TRISCAS})_2$ (4) (top) microscope picture before irradiation of a drop-cast film prepared from a N,N -dimethylformamide solution (bottom) Raman spectrum of the film (red curve) compared to the spectrum measured on a single crystal in the same conditions (green curve).	54
Figure S31. Complex $[\text{Fe}(\text{phen})_3](\Lambda\text{-TRISCAS})_2$ (5) (top) microscope picture before irradiation of a drop-cast film prepared from a N,N -dimethylformamide solution (bottom) Raman spectrum of the film (blue curve) compared to the spectrum measured on a single crystal in the same conditions (green curve).	55
Figure S32. Diffractograms of drop-cast films prepared from N,N -dimethylformamide solutions of complexes $[\text{Fe}(\text{phen})_3](\Delta\text{-TRISCAS})_2$ (4) (top) and $[\text{Fe}(\text{phen})_3](\Lambda\text{-TRISCAS})_2$ (5) (inset in bottom).....	56

Table of compounds

Compound	Space group	Cation	Anion
1·4H ₂ O	<i>oP2₁2₁2</i>	NBu ₄	 $\Delta-1$  $\Delta-1$
2·2CH ₂ Cl ₂	<i>hR32</i> racemic twin		
3·2CH ₂ Cl ₂	<i>hR32</i> racemic twin		
4·2CH ₂ Cl ₂	<i>hR32</i> racemic twin		
4a·2CH ₂ Cl ₂ 4b·MeCN 5b·MeCN	<i>hR32</i>		
5·2CH ₂ Cl ₂	<i>hR32</i> racemic twin		
5b·MeCN 5c·MeCN	<i>hR32</i>		

$6 \cdot 4\text{CH}_2\text{Cl}_2$	<i>mC2/c</i>		
$7 \cdot 4\text{CH}_2\text{Cl}_2 \cdot \text{MeOH}$	<i>hP3₁21</i>		
$8 \cdot \text{CH}_2\text{Cl}_2 \cdot \text{MeOH}$	<i>hP3₂21</i>		
$9 \cdot \text{CH}_2\text{Cl}_2 \cdot \text{MeOH}$	<i>hP3₁21</i> racemic twin		

General comments

CHNS elemental analysis were carried out with an Flash EA1112 ThermoFisher Scientific instr. For Fe, As microanalysis, 5-10 mg of compound were digested with 2 mL of a HNO₃ (70% w/w grade)-HCl (30% w/w grade) (1:1) mixture, diluted to 100 mL. Fe, As contents were then quantified with a Varian ES-720 ICP-OES. Solvents were used freshly distilled under nitrogen: methanol over Mg turnings, CH₂Cl₂ over CaH₂, MeCN over P₂O₅. The infrared spectra were performed on microcrystals powdered samples between 400 and 4000 cm⁻¹ on a SHIMADZU FT-IR spectrophotometer IRPrestige-21 IRAffinity⁻¹ with a iTR™ accessory. All starting materials and reagents were commercially available and used without further purification. All crystallizations were performed under dry argon using standard Schlenk techniques.

X-ray powder diffraction and single crystal data collection and refinement.

Powder X-ray diffraction data were recorded using a PANalytical X'Pert MPD diffractometer

with Bragg-Brentano geometry, Cu K α radiation ($\lambda = 1.54184 \text{ \AA}$) and a backscattering graphite 370 monochromator using standard Al sample holders.

Crystals suitable for X-ray diffraction were mounted to a MiTeGen microloop using Paratone oil for low temperature, and were measured on either on a Bruker KAPPA APEX II for **1, 2, 3, 4, 4a-c, 5, 5b-c, 7, 8 and 9** or on a Bruker-Nonius κ -CCD diffractometer for **6**, operating at 50 kV and 30 mA using graphite monochromated Mo K α ($\lambda = 0.71073 \text{ \AA}$) radiation. Data collection and reduction were performed using SAINT¹ and SADABS² (APEX II), Denzo and Scalepack (KappaCCD) programs.³ Structures were solved by direct methods using SHELXS-97,⁴ SHELXT,⁵ SIR97,⁶ then refined against F² using all data by full-matrix least squares techniques with SHELXL-97 within the WINGX package⁷ or OLEX2⁸. Non-hydrogen atoms were refined anisotropically using weighted full-matrix least-squares on F². All hydrogen atoms positions were generally checked on an Fourier electronic density difference map, then consequently placed at calculated positions and refined using a riding model. Some hydrogen atoms of crystallization water molecules could not be localized, so their positions were calculated with XHYDEX program⁹ or manually fixed at optimized positions and refined using a riding model. All figures were prepared with Mercury¹⁰ and Olex2 softwares. CCDC-1580166 (**Δ -1**), -1580167 (**Δ -1**), -1580168 (**rac-1**), -1580170 (*rac*-TRISCAS.NBu₄), -1580172 (**2**), -1580178 (**3**), -1580173 (**4**), -1580174 (**4a**), -1580181 (**4b**), -1580177 (**4c**), -1580176 (**5**), -1580180 (**5b**), -1580179 (**5c**), -764110 (**6**), -1580171 (**7**), -1580169 (**8**) and -1580175 (**9**) contain the supplementary crystallographic data for this paper. These data can be obtained free of charge via www.ccdc.cam.ac.uk/data_request/cif, or by emailing data_request@ccdc.cam.ac.uk, or by

¹ Bruker, SAINT. Bruker AXS Inc., 2012, Madison, Wisconsin, USA.

² G. M. Sheldrick. SADABS. Program for Empirical Absorption Correction. 1996, University of Gottingen, Germany.

³ Z. Otwinowski and W. Minor "Processing of X-ray Diffraction Data Collected in Oscillation Mode", Methods in Enzymology, Volume 276: Macromolecular Crystallography, part A, p. 307-326, 1997, C.W. Carter, Jr. and R.M. Sweet, Eds., Academic Press.

⁴ G. M. Sheldrick *Acta Cryst. A*, 2008, 64, 112.

⁵ G. M. Sheldrick *Acta Cryst. A*, 2015, 71, 3.

⁶ Altomare, A.; Burla, M. C.; Camalli, M.; Cascarano, G. L.; Giacovazzo, C.; Guagliardi, A.; Moliterni, A. G. G.; Polidori, G.; Spagna, R. *J. Appl. Cryst.*, 1999, 32, 115

⁷ L.J. Farrugia *J. Appl. Cryst.*, 1999, 32, 837.

⁸ O. V. Dolomanov, L. J. Bourhis, R. J. Gildea, J. A. K. Howard, H. Puschmann *J. Appl. Crystallogr.*, 2009, 42, 339.

⁹ A. G. Orpen *J. Chem. Soc., Dalton Trans.*, 1980, 2509.

¹⁰ MERCURY CSD 3.8: C. F. Macrae, I. J. Bruno, J. A. Chisholm, P. R. Edgington, P. McCabe, E. Pidcock, L. Rodriguez-Monge, R. Taylor, J. van de Streek, P. A. Wood *J. Appl. Cryst.*, 2008, 41, 466.

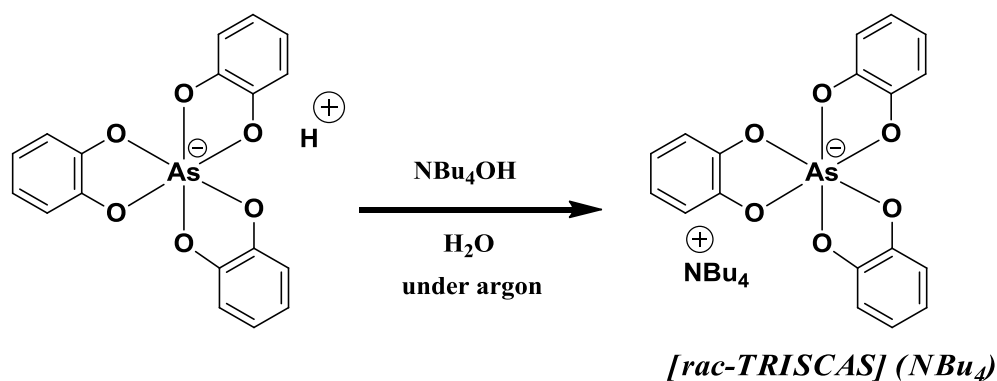
contacting The Cambridge Crystallographic Data Centre, 12, Union Road, Cambridge CB2 1EZ, UK; fax: +44 1223 336033.

Salts of chiral anions

Synthesis

Tris(o-phenylenedioxy)phosphate(V) (TRISCAT) tributylammonium was synthesized adapting the literature procedure for TRISPHAT¹¹ using catechol instead of 3,4,5,6-tetrachlorobenzene-1,2-diol.

The synthesis of racemic tris(o-phenylenedioxy)arsenate(V) (TRISCAS) tetrabutylammonium was performed according to the following procedure (**Scheme S1**) : 10 grams (20 mmol) of racemic acid of TRISCAS were dissolved in 100 mL of deionized water under argon. The addition to the reaction flask of a solution of NBu₄OH (11.00 mL, 1.84 M) that was previously carefully titrated, resulted directly in the evolution of a white solid. The reaction was then stirred for one hour under argon at room temperature and placed in ice for 30 min to ensure the complete precipitation of the product. The white solid product was collected and dried under vacuum. The product was recrystallized from ethanol to remove impurities. X-ray diffraction on one crystal evidenced the formation of the product (see corresponding cif file). The total yield of the reaction based on the initial amount of H(TRISCAS) was 70% (~9.00 g). Elemental analysis for C₃₄H₄₈AsNO₆(EtOH)_{0.5} (664.70 g.mol⁻¹) : calculated C 63.24, H 7.73, N 2.10; experimental C 63.37, H 7.97, N 2.16.



Scheme S1. Synthesis of lipophilic racemic- tris(o-phenylenedioxy)arsenate(V) (TRISCAS) tetrabutylammonium.

¹¹ F. Favarger, C. Goujon-Ginglinger, D. Monchaud, J. Lacour *J. Org. Chem.*, **2004**, *69*, 8521.

The Δ/Λ tris(o-phenylenedioxy)arsenate(V) (TRISCAS) salts,¹² and racemic/ Δ tris(tetrachlorobenzenediolato) phosphate (V) (TRISPHAT) salts,¹¹ were prepared following literature procedures. $K_2[\Delta\text{-Sb}_2(\text{tartrate})_2]$ and $K_2[\Lambda\text{-Sb}_2(\text{tartrate})_2]$ were prepared straightforwardly by boiling a 1:2:2 mixture of Sb_2O_3 , tartaric acid and KOH in water.¹³

General synthesis for **1**. Previously titrated tetrabutylammonium hydroxide (20 mmol) was added to a flask containing As_2O_3 (1.97 g, 10 mmol). The suspension was stirred for 20 min until the arsenic trioxide was dissolved. To the resulting solution was added an equimolar amount of D(-)-tartaric acid and/or L(+)-tartaric acid dissolved in 50 mL H_2O . After stirring a few minutes, a white solid started to precipitate. The reaction was stirred for 48 h at r.t. The precipitate was filtered and recrystallized from acetone yielding large crystals that were isolated and dried under vacuum.

$(\text{NBu}_4)_2[\text{rac-As}_2(\text{tartrate})_2]$, **rac-1**. Yield: 68% (6.31 g). Elemental analysis calc. for $\text{C}_{40}\text{H}_{76}\text{As}_2\text{N}_2\text{O}_{12}(\text{H}_2\text{O})_{3.5}$ (989.93 $\text{g}\cdot\text{mol}^{-1}$) C 48.53, H 8.45, N 2.82; found C 48.58, H 8.62, N 2.94. IR (ATR, cm^{-1}): 2964w, 2939w, 2922w, 2877w, $[\nu(\text{C-H})]$; 1662s(sh), 1646s $[\nu(\text{C=O})]$; 1486m, 1354s $[\delta(\text{C-H})]$; 1125m $[\nu(\text{C-O})]$.

$(\text{NBu}_4)_2[\Delta\text{-As}_2(\text{tartrate})_2]$, **Δ -1**. Yield 70% (6.45 g). Elemental analysis calc. for $\text{C}_{40}\text{H}_{76}\text{As}_2\text{N}_2\text{O}_{12}(\text{H}_2\text{O})_{3.3}$ (986.33 $\text{g}\cdot\text{mol}^{-1}$) C 48.70, H 8.44, N 2.84; found C 48.60, H 8.63, N 2.91. IR (ATR, cm^{-1}): 2964w, 2935w, 2877w $[\nu(\text{C-H})]$; 1662s(sh), 1652s, 1645s(sh), 1635s(sh) $[\nu(\text{C=O})]$; 1486m, 1341s $[\delta(\text{C-H})]$; 1125m $[\nu(\text{C-O})]$.

$(\text{NBu}_4)_2[\Lambda\text{-As}_2(\text{tartrate})_2]$, **Λ -1**. Yield 83% (7.26 g). Elemental analysis calc. for $\text{C}_{40}\text{H}_{76}\text{As}_2\text{N}_2\text{O}_{12}(\text{H}_2\text{O})_{2.5}$ (971.93 $\text{g}\cdot\text{mol}^{-1}$) C 49.43, H 8.40, N 2.88; found C 49.37, H 8.16, N 2.98. IR (ATR, cm^{-1}): 2961w, 2938w, 2875w $[\nu(\text{C-H})]$; 1662s(sh), 1660s, 1653s $[\nu(\text{C=O})]$; 1485m, 1332s $[\delta(\text{C-H})]$; 1124m $[\nu(\text{C-O})]$.

¹² A. Rosenheim, W. Plato *Ber. Dtsch. Chem. Ges. B*, **1925**, 58, 2000. G. E. Ryschkewitsch, J. M. Garrett *J. Am. Chem. Soc.*, **1968**, 90, 7234.

¹³ H. Schmidt, *Z. Ang. Chem.*, **1930**, 44, 963.

Specific rotation values, at $[\alpha]_D^{25} = +34.0(10)/-33.2(5)^\circ$ for Λ/Δ -**1** (acetonitrile, $0.01 \text{ g}\cdot\text{mL}^{-1}$), were rather low compared to commercially available $\text{K}_2[(+)\text{-Sb}_2(\text{tartrate})_2]\cdot x\text{H}_2\text{O}$ ($[\alpha]_D^{25} = +138.1(5)^\circ$ in water)¹⁴ or the previously reported $\text{K}_2[(+)\text{-As}_2(\text{tartrate})_2]$ ($[\alpha]_D^{25} = +85.5^\circ$ in water)¹⁵. They are closer to values for tartaric acid,¹⁶ raising doubts about whether the adduct structure is wholly maintained in solution. The comparison of FTIR in the solid state and in THF solution (see below Figure S5) evidences that low specific rotation values in solution are caused by the loss of D_2 -symmetry for the chiral anion towards partly coordinated species. Surprisingly this dissociation was not observed by NMR, possibly due to a difference in experimental time-scale.¹⁷ Nevertheless, recrystallization of the anion with good yields demonstrated a return to the D_2 chiral structure in the solid state and thus a reversibility of the dissociation process.

¹⁴ Sigma-Aldrich commercial product $[\alpha]_D^{25}$ given as $+141^\circ$, measured in water, $c = 22.23(4)\text{g/L}$, with a 20 cm optical path cell.

¹⁵ Schlessinger, G. SODIUM (+)-ARSENYL TARTRATE. *Inorg. Synth.* **1970**, *12*, 267–268.

¹⁶ Gawronski, J.; Gawronska, K. Tartaric Acid and Its Salts. In *Tartaric and Malic Acids in Synthesis*; John Wiley&Sons, 1999; pp 1–11.

¹⁷ Marcovich, D.; Tapscott, R. E. ^{13}C NMR Studies on Arsenic(III) and Antimony(III) Dihydroxydicarboxylate Complexes Dragoslav. *J. Am. Chem. Soc.* **1980**, No. 102, 5712–5717.

Crystallographic data for **1**

Colourless single crystals were selected from batches of Δ -**1**, Λ -**1** and *rac*-**1** and diffraction data were collected at 120 K. The structures of **1** are all isostructural in the Sohncke $P2_12_12$ space group. The structures of Δ -**1** and Λ -**1** show high optical purity as evidenced by the Flack parameter (0.011(4) and 0.024(4), respectively). For *rac*-**1** the structure was refined as an inversion twin with a Flack parameter of 0.010(9), demonstrating the coexistence of isochiral domains at the microscopic level, and the occurrence of an arsenic template effect: the isomer with two homochiral tartrates is favoured, due to steric hindrance in the heterochiral arrangement.¹⁸

The structures are composed of the arsenyl tartrate anion surrounded by two NBu_4 cations and four water molecules. The water molecules are localized in the void spaces of the lattice, and are part of a hydrogen bond network between the oxygen atoms of the tartrate and the hydrogen atoms of the tetrabutylammonium cation, as shown below.

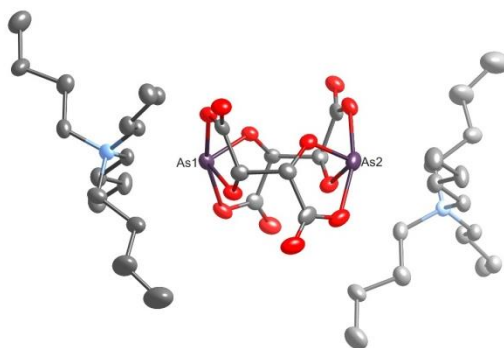


Figure S2. Asymmetric unit of Δ -**1** at 120 K.

¹⁸ Marcovich, D.; Tapscott, R. E. ¹³C NMR Studies on Arsenic(III) and Antimony(III) Dihydroxydicarboxylate Complexes Dragoslav. *J. Am. Chem. Soc.* **1980**, No. 102, 5712–5717.

	(NBu ₄) ₂ [Δ -As ₂ (tartrate) ₂] ·4H ₂ O	(NBu ₄) ₂ [Λ -As ₂ (tartrate) ₂] ·4H ₂ O	(NBu ₄) ₂ [<i>rac</i> -As ₂ (tartrate) ₂] ·4H ₂ O
Formula		C ₄₀ H ₇₄ As ₂ N ₂ O ₁₆	
Formula weight (g·mol ⁻¹)		988.85	
Crystal color		colorless	
Crystal size (mm)	0.36×0.06×0.06	0.2×0.06×0.04	0.38×0.30×0.22
<i>T</i> (K)		120(2)	
Wavelength (Å)		0.71073	
Crystal system		Orthorhombic	
Space group		<i>oP</i> 2 ₁ 2 ₁ 2	
<i>a</i> (Å)	21.0850(14)	21.099(2)	21.148(4)
<i>b</i> (Å)	22.5516(15)	22.521(3)	22.484(4)
<i>c</i> (Å)	10.4629(7)	10.4663(12)	10.4604(17)
<i>V</i> (Å ³)	4975.1(6)	4973.4(10)	4973.8(15)
<i>Z</i>		4	
ρ_{calc} (g·cm ⁻³)	1.32	1.321	1.321
μ (mm ⁻¹)	1.407	1.408	1.408
F(000)		2088	
θ range (°)	3.328 ≤ θ ≤ 21.75	3.606 ≤ θ ≤ 27.998	2.885 ≤ θ ≤ 27.52
Index ranges	-21 ≤ <i>h</i> ≤ 21 -23 ≤ <i>k</i> ≤ 23 -10 ≤ <i>l</i> ≤ 10	-27 ≤ <i>h</i> ≤ 27 -29 ≤ <i>k</i> ≤ 29 -13 ≤ <i>l</i> ≤ 13	-27 ≤ <i>h</i> ≤ 27 -29 ≤ <i>k</i> ≤ 29 -13 ≤ <i>l</i> ≤ 13
Total refls.	51447	80709	105145
Absorption correction		Sadabs	
<i>T</i> _{min} , <i>T</i> _{max}	0.628, 0.745	0.656, 0.746	0.554, 0.746
Unique refls. (<i>I</i> > 2 σ (<i>I</i>))	5172	8641	10051
Completeness (θ =25.19°, %)	0.992	0.97	0.993
<i>R</i> _{int}	0.062	0.0883	0.0504
Refined param./restr.	560/3	554/0	560/0
Final <i>R</i> indices (<i>I</i> > 2 σ (<i>I</i>))	<i>R</i> 1=0.0318 w <i>R</i> 2=0.0751	<i>R</i> 1=0.0574 w <i>R</i> 2=0.1092	<i>R</i> 1=0.0396 w <i>R</i> 2=0.0908
<i>R</i> indices (all data)	<i>R</i> 1=0.0419 w <i>R</i> 2=0.0791	<i>R</i> 1=0.0912 w <i>R</i> 2=0.1187	<i>R</i> 1=0.0486 w <i>R</i> 2=0.0946
Goodness-of-fit (<i>S</i>)	1.048	1.041	1.059
(Δ / σ) _{max}	0.007	0.001	0.001
$\Delta\rho_{\text{max}} / \Delta\rho_{\text{min}}$ (e ⁻ Å ⁻³)	0.57/-0.24	0.78/-0.71	0.90/-0.49
Flack parameter	0.011(4)	0.024(4)	0.010(9)
Friedel coverage	0.996	0.972	0.999

Table S3. Crystallographic data for (NBu₄)₂[As₂(tartrate)₂]·4H₂O, Δ -1, Λ -1 and *rac*-1.

Arsenic are represented in purple, oxygen in red, nitrogen in blue, carbon in grey. Water molecules were omitted for clarity, displacement ellipsoids are displayed at 50% probability.

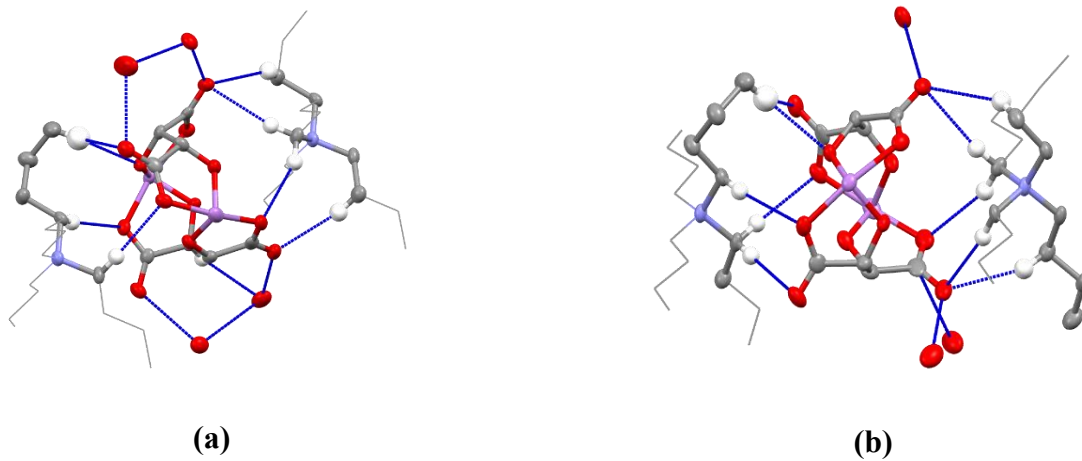


Figure S4. Hydrogen bonding between butyl chains and oxygen atoms of hydroxyles/carboxyles of the anion and water molecules for **1**.

(a) $(\text{NBu}_4)_2[\Delta\text{-As}_2(\text{tartrate})_2]$; (b) $(\text{NBu}_4)_2[\Lambda\text{-As}_2(\text{tartrate})_2]$. Short contacts are shown in blue.

Infrared data

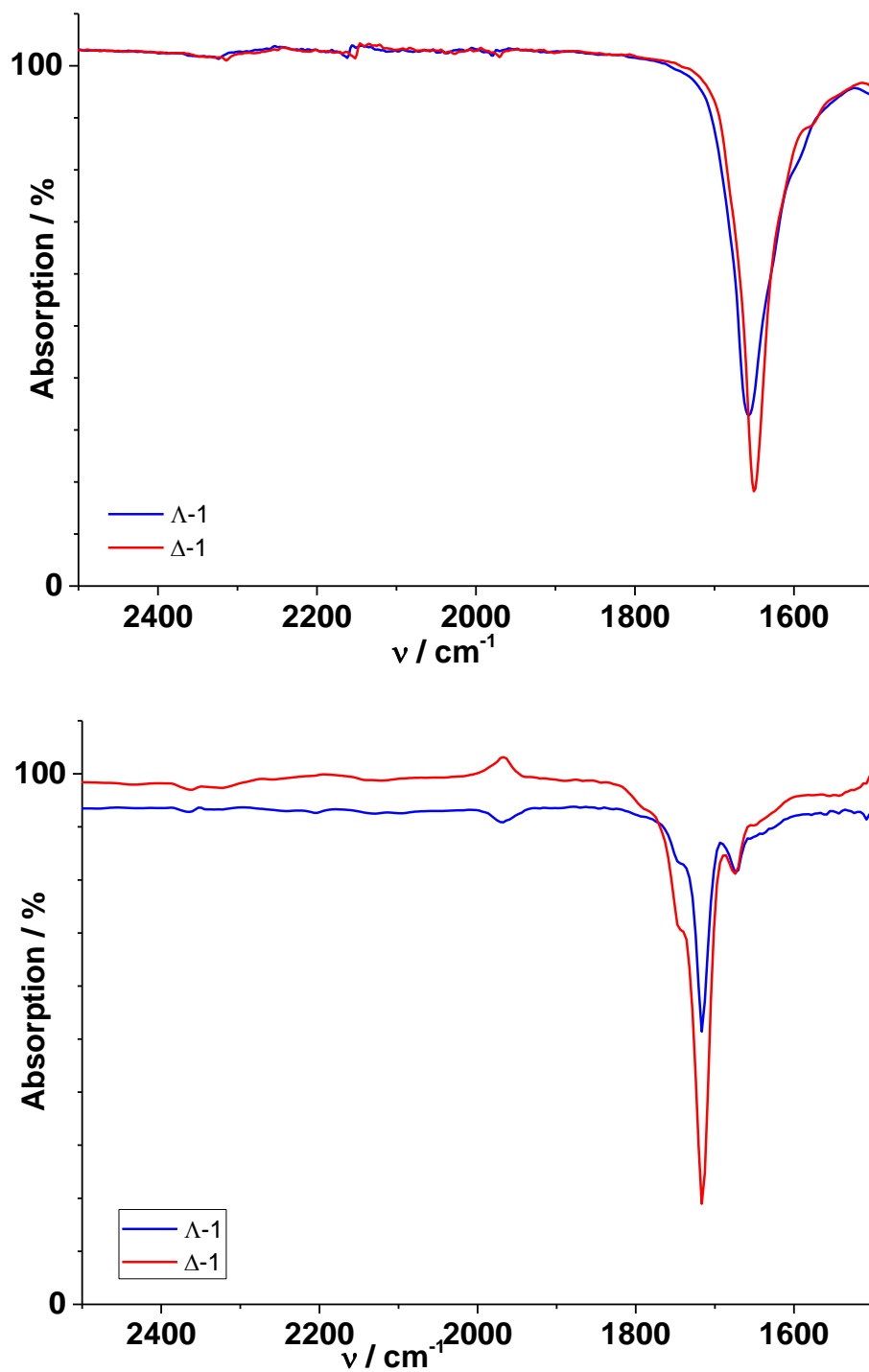


Figure S5. FTIR spectra of (NBu₄)₂[Λ-As₂(tartrate)₂] (blue line) Λ-1 and (NBu₄)₂[Δ-As₂(tartrate)₂] (red line) Δ-1 in the solid state (top) and in solution in THF (bottom).

The carbonyl vibrational modes of arsenic and antimony tartrate derivatives were reported to split and shift to lower frequencies (1670 and 1620 cm⁻¹) compared to free (+)-tartaric acid (1740 cm⁻¹)

¹).¹⁹ Indeed we found that FTIR for Δ -**1** and Λ -**1** in the solid state show $\nu(\text{C}=\text{O})$ stretching at 1650 cm^{-1} and 1656 cm^{-1} respectively. However, spectra of Δ/Λ -**1** in wet THF show similar spectra with two weak bands about 1745 cm^{-1} and at 1674 cm^{-1} , and a strong band at 1717 cm^{-1} . The two bands above 1710 cm^{-1} are assigned to tartaric acid species having uncoordinated carboxyl groups, the lower energy band to the coordinated tartrate. Overall no bands corresponding to free tartrate are observed.²⁰

¹⁹ Bott, R. C.; Smith, G.; Sagatys, D. S.; Lynch, D. E.; Kennard, C. H. L. *Aust. J. Chem.* **2000**, *53*, 917

²⁰ Brizard, A.; Berthier, D.; Aimé, C.; Buffeteau, T.; Cavagnat, D. ; Ducasse, L. ; Huc, I. ; Oda, R. *Chirality*, **2009**, *21*, 153.

Complexes

Synthesis of complexes 2-5

[Fe(phen)₃](TRISCAT)₂ (2). over a freshly prepared solution of 1,10-phenanthroline (216 mg, 1.20 mmol) and [TRISCAT(HNBu₃)] (433 mg, 0.80 mmol) in 4 mL of distilled dichloromethane in a Schlenck tube under argon, were layered 5 mL of a 1:1 CH₂Cl₂/MeOH mixture and then Fe(H₂O)₇(SO₄) (111 mg, 0.40 mmol) in 10 mL MeOH. After a few weeks, red plate single crystals were obtained, then filtered and washed with cold methanol. Yield: 380 mg (65%) . Elemental Anal. Calcd. (%) for C₇₂H₄₈P₂FeN₆O₁₂(CH₂Cl₂)_{1.1}(H₂O)₃ (1454.44 g/mol): C 60.36; H 3.89; N 5.77. Found (%): C 60.38; H 3.76; N 5.71. IR (ATR, cm⁻¹): 3071w, 3055w, 3036w [ν(C–H) aromatic]; 1647w, 1632w, [ν(C=N)imine]; 1600w, 1578w, 1512w, 1485m [ν(C=C)aromatic]; 1427w, 1412w, 1354w, 1246m, 1211m, 1146w, 1099w [δ(C–H), ν(C–O)]; 1011w, 980w, 941w, 907w, 875w, 841w, 822m, 725s, 667m [δ (=C–H), δ(C–H)].

Structure determination of the red plates showed an asymmetric unit containing one sixth of a Fe(II) cation, with the Fe atom lying on the intersection between crystallographic twofold and threefold axes, and one third of the phosphate counter anion with the phosphorus lying on the same threefold axis. Out of the residual electronic density difference map a disordered dichloromethane molecule could be identified and modelled, with one chlorine atom lying on a crystallographic threefold axis.

[Fe(phen)₃](rac-TRISCAS)₂ (3). Fe(H₂O)₇(SO₄) (100 mg, 0.35 mmol) in 5 mL MeOH together with a little amount of ascorbic acid was mixed in a Schlenck tube under argon with freshly prepared solutions of 1,10-phenanthroline (193 mg, 1.07 mmol) in 5 mL CH₂Cl₂ and (TRISCAS)NBu₄ (456 mg, 0.71 mmol) in 7 mL CH₂Cl₂. After a few days, red microcrystalline powder together with red cubic single crystals were obtained, then filtered and washed with cold methanol. Yield: 235 mg (42%). Elemental Anal. Calcd. (%) for C₇₂H₄₈As₂FeN₆O₁₂(H₂O)_{1.5}(CH₂Cl₂)_{1.7} (1566.280 g/mol): As 9.56; Fe 3.56; C 56.51; H 3.50; N 5.36. Found (%): As 9.38; Fe 3.75; C 56.53; H 3.49; N 5.53. IR (ATR, cm⁻¹): 3066w, 3028w [ν(C–H) aromatic]; 1631w [ν(C=N)imine]; 1593w, 1577w, 1516w, 1477s [ν(C=C)aromatic]; 1427m, 1334w, 1238s, 1203m, 1149w, 1099m [δ(C–H), ν(C–O)]; 1014w, 910w, 875w, 864w, 794s, 736s, 721s, 667s[δ (=C–H), δ(C–H)].

[Fe(phen)₃](Δ-TRISCAS)₂ (4). a freshly prepared solution of 1,10-phenanthroline (193 mg, 1.07 mmol) and (Δ-TRISCAS)cinchoninium (493 mg, 0.71 mmol; d.e = 88 %) in 10 mL of a 1:1 CH₂Cl₂/methanol mixture in a Schlenck tube under argon was layered over with 5 mL of a 1:1 CH₂Cl₂/MeOH mixture then with a solution of Fe(H₂O)₇(SO₄) (100 mg, 0.35 mmol) in 5 mL MeOH. After a few weeks, clear intense red prismatic single crystals were obtained, then filtered and washed with cold methanol. Yield : 440 mg (81%). Elemental Anal. Calcd. (%) for C₇₂H₄₈As₂FeN₆O₁₂(H₂O)_{1.3}(CH₂Cl₂)_{1.7} (1562.677 g/mol): As 9.58; Fe 3.57; C 56.64; H 3.48; N 5.37. Found (%): As 9.62; Fe 3.83; C 56.66; H 3.42; N 5.43. IR (ATR, cm⁻¹): 3067w, 3028w [ν(C-H) aromatic]; 1631w [ν(C=N)_{imine}]; 1593w, 1578w, 1516w, 1477s [ν(C=C)aromatic]; 1427m, 1334w, 1238s, 1204m, 1149w, 1099m [δ(C-H), ν(C-O)]; 1015w, 910w, 876w, 864w, 795s, 737s, 721s, 667s [δ(=C-H), δ(C-H)].

[Fe(phen)₃](Δ-TRISCAS)₂ (4a) was prepared using analogous procedure as **3** but the diastereomeric excess of Δ-TRISCAS salt used was 86%.

[Fe(phen)₃](Λ-TRISCAS)₂ (5). Fe(H₂O)₇(SO₄) (100 mg, 0.35 mmol) in 5 mL MeOH together with a little amount of ascorbic acid was mixed in a Schlenck tube under argon with freshly prepared solutions of 1,10-phenanthroline (193 mg, 1.07 mmol) in 5 mL CH₂Cl₂ and (Λ-TRISCAS)cinchonidinium (493 mg, 0.71 mmol; d.e=66%) in 7 mL CH₂Cl₂. After a few days, red microcrystalline powder together with red prismatic single crystals were obtained, then filtered and washed with cold methanol. Yield : 372 mg (68%) Elemental Anal. Calcd. (%) for C₇₂H₄₈As₂FeN₆O₁₂(H₂O)_{0.5}(CH₂Cl₂)_{1.5} (1562.677 g/mol): C 57.65; H 3.42; As 9.79; Fe 3.65; N 5.49. Found (%): C 57.64; H 3.36; As 9.44; Fe 3.95; N 5.60. IR of **5** (ATR, cm⁻¹): 3075w, 3030w [ν(C-H) aromatic]; 1631w [ν(C=N)_{imine}]; 1592w, 1580w, 1515w, 1478s [ν(C=C)aromatic]; 1429m, 1413m, 1333w, 1238s, 1204m, 1152w, 1143w, 1099m [δ(C-H), ν(C-O)]; 1059w, 1015m, 983w, 943w, 909m, 877m, 866m, 798s, 768m, 741-718s, 672-659s [δ(=C-H), δ(C-H)]

Crystallographic data for complexes 2-5

hkl data for complex **4** integrated in trigonal settings, scaled and merged in the P1 point group, was analyzed in the following way by Prof. Flack:

15833 measured data intensities come from a set of raw data containing 52987 reflections. The file contains *h k l* $|F_{\text{obs}}|^2$ u. No $|F_{\text{model}}|^2$ were used in the following. Cell reduction indicates that the crystal structure has Bravais-lattice type hR. There are five point groups belonging to hR: $-3m$, 32 , $3m$, -3 and 3 . These cover two Laue classes (i.e. $-3m$ and -3).

Special (i.e. ones which are not general) reflections of point group $-3m$ were set aside. The intensity data were assembled into sets of reflections symmetry-equivalent under point group $-3m$. There are 12 (general) symmetry-equivalent reflections in point group $-3m$. Only those sets where all 12 reflections had been measured were used in the following analysis. The incomplete sets were set aside. There were 45 sets of $-3m$ -general reflections in the data corresponding to 540 reflections. R_{merge} values on $|F_{\text{obs}}|^2$, A and D were calculated separately for the five point groups [A and D are the average and difference of Friedel opposites]. The results are given in the following table.

	$-3m$	32	$3m$	-3	3
$R_{ F_{\text{obs}} ^2}$ (%)	1.79	0.94	1.74	1.77	0.80
R_A (%)	0.60	0.60	0.60	0.50	0.50
R_D (%)	100	55.2	348	100	44.1

Table S6. Point group analysis for complex **4**.

The results are very much in line both with those of KH(2R,3R)tartrate measured by Phil Pattison and the least-squares refinements on this compound.

[1] With the measurement procedure used, 52987 raw reflections gave 15833 when merged and averaged in point group 1, resulting in only 45 complete sets of 12 $-3m$ general reflections (i.e. 540 reflections). So whilst the "ordinary" measurement protocols are satisfactory for "ordinary" structure solution and refinement, they do not provide optimal data sets for the use in analyses like those undertaken here on complex **4**. 45 complete sets are really too few.

[2] The R_{merge} values on A and D are clearly far more discriminating than those on $|F_{\text{obs}}|^2$. [We already knew that, as with KH(2R,3R)tartrate, the resonant scattering signal in the intensity data was clearly visible.] Looking at R_D , there is little to choose between point groups 3 and

32. 44% and 55% are really low values for R_D merge. R_D of $3m$ is super high. Both Laue classes have very decently low values of R_A .

Datasets for complexes **3** and **4** were integrated and scaled in the 3 point group. Structures could be solved in the *R3* and *R32* space groups. Refinement provided consistently better results with the latter. The refinement was done without the TWIN instruction and further analyzed by Prof. Flack.

Numerical values of a Flack (2013) style analysis²¹ are given in the table below, with appropriate plots following.

	Complex 3	Complex 4
Friedif _{stat}	734	734
Friedif _{obs}	214	396
Friedif _{single}	568	562
R _A %	4.8	5.2
R _D %	334	52.0
RAweak %	11.9	7.1
Reflection count		
Friedel pairs	1520	1561
Centric	353	356
Unpaired acentric	30	1
Total	3423	3479
Flack parameter		
from slope of selected D plot	0.40921(8)	0.15995(5)
from LS refinement with twin law	0.429(2)	0.1724(18)

²¹ H. D. Flack *Acta Cryst. C*, **2013**, *69*, 803.

As can be seen, the Friedif_{stat} value at 734 shows that resonant scattering effects are important in complexes **3** and **4** as expected with the heavy atoms present. For complex **3**, one reflection is an obvious outlier for D and has been omitted.

Conclusion: These two crystals are definitely twinned by inversion. The proportions of the twins found by refinement of the Flack parameter including the twin law and those deduced from the slope of the selected-D plot correspond very closely indeed.

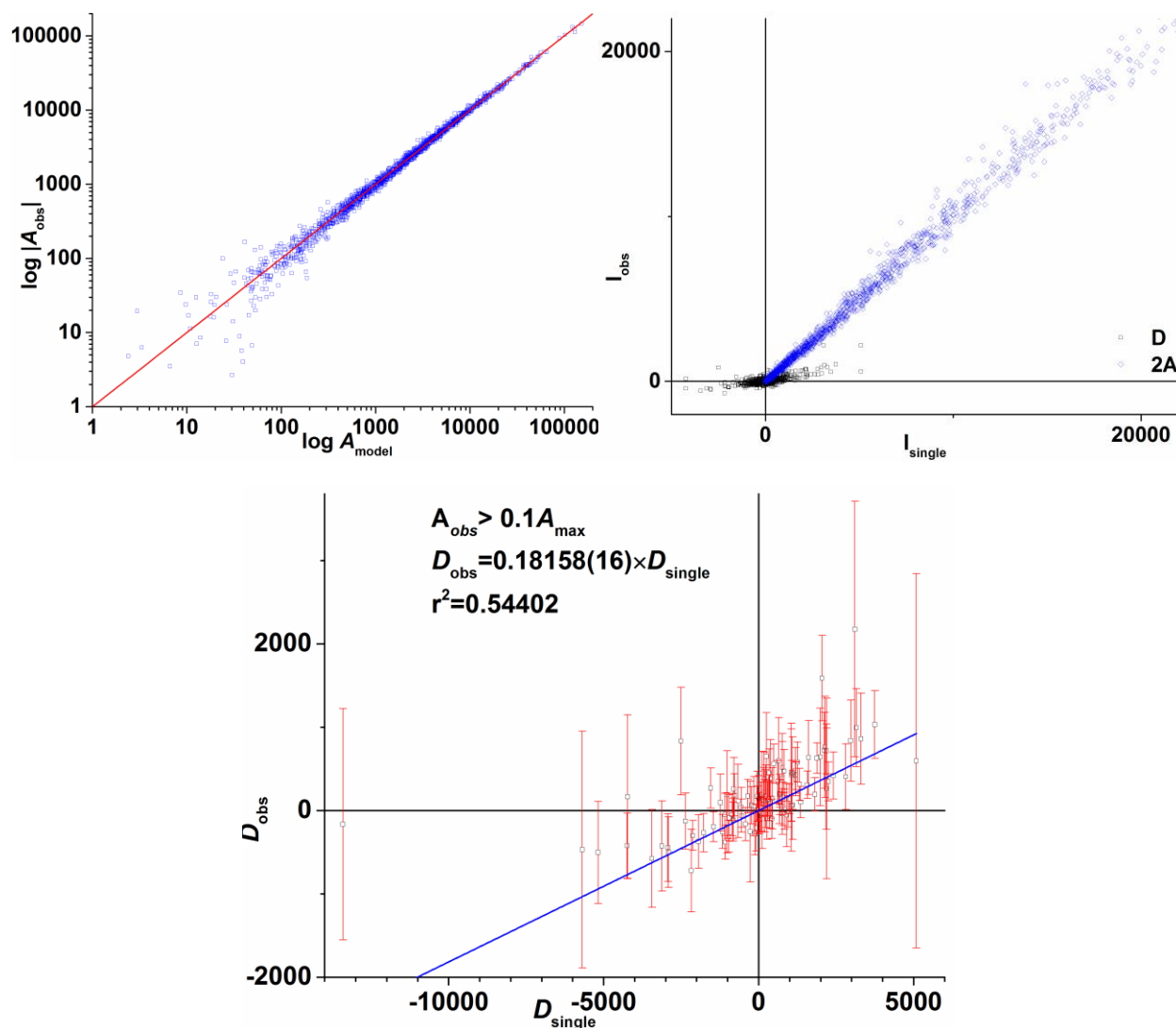


Figure S7. Plots of $(A_{\text{model}}, A_{\text{obs}})$, 2AD and Flack parameter determination from $(D_{\text{single}}, D_{\text{obs}})$ for complex **3**.

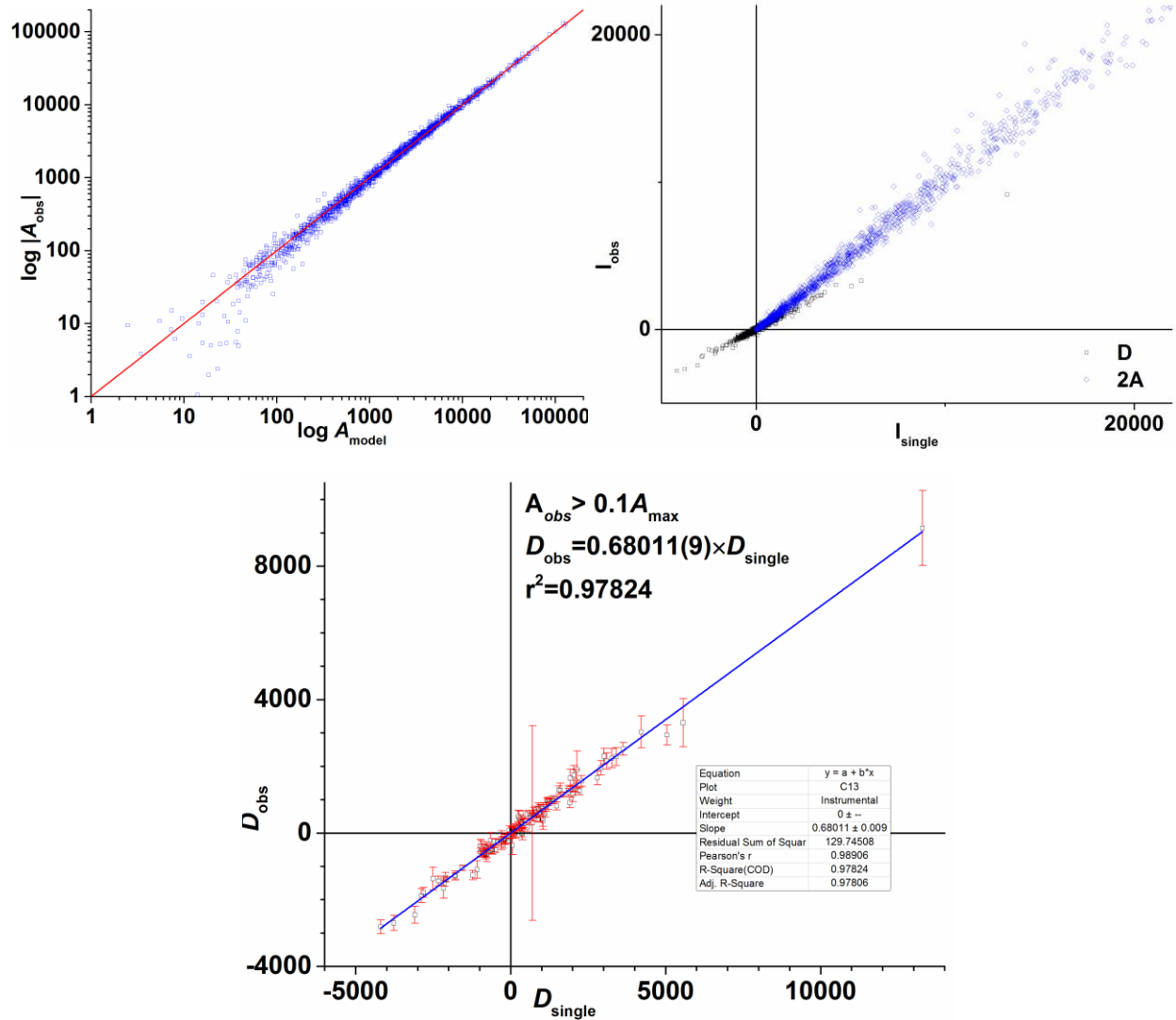


Figure S8. Plots of $(A_{\text{model}}, A_{\text{obs}})$, 2AD and Flack parameter determination from $(D_{\text{single}}, D_{\text{obs}})$ for complex 4.

Complex	Complex 2	Complex 3	Complex 4	Complex 4a	Complex 5
	[Fe(<i>phen</i>) ₃](rac-TRISCAT) ₂	[Fe(<i>phen</i>) ₃](rac-TRISCAS) ₂	[Λ-Fe(<i>phen</i>) ₃](Δ-TRISCAS) ₂	[Λ-Fe(<i>phen</i>) ₃](Δ-TRISCAS) ₂	[Λ-Fe(<i>phen</i>) ₃](Λ-TRISCAS) ₂
Formula	C ₇₄ H ₅₂ Cl ₄ FeN ₆ O ₁₂ P ₂			C ₇₄ H ₅₂ As ₂ Cl ₄ FeN ₆ O ₁₂	
Formula weight (g.mol ⁻¹)	1476.8			1564.70	
Crystal color	dark red			dark red	
Crystal size (mm)	0.46×0.3×0.06	0.08×0.15×0.1	0.17×0.35×0.5	0.2×0.2×0.04	0.34×0.09×0.09
<i>T</i> (K)			120(2)		
Wavelength (Å)			0.71073		
Crystal system			Trigonal		
Space group			<i>hR32</i>		
<i>a</i> (Å)	15.1311(5)	15.147(4)	15.1470(3)	15.142(5)	15.153(1)
<i>c</i> (Å)	25.4797(9)	25.656(7)	25.6659(5)	25.630(8)	25.660(5)
<i>V</i> (Å ³)	5052.0(4)	5097(3)	5099.6(2)	5089(3)	5102.5(14)
<i>Z</i>			3		
ρ _{calc} (g·cm ⁻³)	1.456	1.533	1.528	1.532	1.528
μ (mm ⁻¹)	0.5	1.414	1.414	1.417	1.413
F(000)	2274	2382	2382	2382	2382
θ range (°)	1.755 ≤ θ ≤ 27.499	1.755 ≤ θ ≤ 27.499	4.186 ≤ θ ≤ 34.061	2.222 ≤ θ ≤ 30.811	2.22 ≤ θ ≤ 27.523
Index ranges	-23 ≤ h ≤ 22	-22 ≤ h ≤ 21	-21 ≤ h ≤ 23	-21 ≤ h ≤ 20	-19 ≤ h ≤ 19
	-24 ≤ k ≤ 24	-21 ≤ k ≤ 22	-22 ≤ k ≤ 23	-21 ≤ k ≤ 21	-19 ≤ k ≤ 19
	-39 ≤ l ≤ 40	-35 ≤ l ≤ 36	-30 ≤ l ≤ 39	-35 ≤ l ≤ 36	-33 ≤ l ≤ 33
Total refls.	46589	55642	53905	1.417	55868
Absorption correction			Sadabs		
<i>T</i> _{min} , <i>T</i> _{max}	0.665, 0.7469	0.7719, 0.8375	0.912, 1.000	0.7511, 0.8622	0.6605, 0.7456
Unique refls. (<i>I</i> > 2σ(<i>I</i>))	4445	3487	4045	3003	2519
Completeness (θ=25.19°, %)	99.7	99.4	99.3	99.9	99.9
<i>R</i> _{int}	0.057	0.0292	0.0229	0.0378	0.0394
Refined param./restr.	162/0	163/0	163/0	162/0	162/0
Final <i>R</i> indices (<i>I</i> > 2σ(<i>I</i>))	<i>R</i> 1=0.0516	<i>R</i> 1=0.0387	<i>R</i> 1=0.0370	<i>R</i> 1=0.0397	<i>R</i> 1=0.0372
	w <i>R</i> 2=0.1531	w <i>R</i> 2=0.1057	w <i>R</i> 2=0.1078	w <i>R</i> 2=0.1072	w <i>R</i> 2=0.1024
	<i>R</i> 1=0.057	<i>R</i> 1=0.0463	<i>R</i> 1=0.0393	<i>R</i> 1=0.0492	<i>R</i> 1=0.0386
<i>R</i> indices (all data)	w <i>R</i> 2=0.1575	w <i>R</i> 2=0.1095	w <i>R</i> 2=0.1097	w <i>R</i> 2=0.1124	w <i>R</i> 2=0.1035
Goodness-of-fit on <i>F</i> ²	1.084	1.063	1.074	1.057	1.061
(Δ / σ) _{max}	0	0.001	0.001	0.001	0.001
Δρ _{max} / Δρ _{min} (e ⁻ Å ⁻³)	0.967/-2.044	0.898/-1.734	0.996/-1.896	0.838/-1.628	0.802/-1.374
Flack parameter	0.45(2)	0.473(15)	0.163(13)	-0.006(3)	0.277(2)
Friedel coverage	0.999	1	0.998	1	1

Friedel coverage is calculated by Shelxl as the number of unique Friedel pairs measured divided by the number that would be possible theoretically, ignoring centric projections and systematic absences.

Table S9. Crystallographic data for complexes 2-5.

complex	Complex 2	Complex 3	Complex 4a	Complex 5
	[Fe(<i>phen</i>) ₃](rac-TRISCAT) ₂	[Fe(<i>phen</i>) ₃](rac-TRISCAS) ₂	[Λ-Fe(<i>phen</i>) ₃](Δ-TRISCAS) ₂	[Δ-Fe(<i>phen</i>) ₃](Λ-TRISCAS) ₂
<i>Fe-N_{av}</i>	1.9680(14)	1.9716(18)	1.971(2)	1.972(3)
<i>Fe-As(or P)_(triad)</i>	5.6889(8)	5.7162(16)	5.7104(19)	5.7182(12)
<i>Fe-As(or P)_(shell)</i>	9.1750(4)	9.1932(11)	9.1893(14)	9.1961(6)
<i>As(or P)_(shell) – As(or P)_(shell)</i>	10.3815(9)	10.4227(8)	10.4173(16)	10.4250(10)
<i>C-H_(α-acidic)•••O_(anion)</i>	3.273(3)	3.266(3)	3.266(6)	3.272(6)
<i>C-H•••C_(π)</i>	3.499(4)	3.531(5)	3.530(6)	3.534(6)
<i>O_(π)•••C_(π)</i>	3.104(4)	3.107(4), 3.236(6)	3.107(5), 3.205(7)	3.109(6), 3.207(6)

Table S10. Average distances and interactions (Å) for complexes 2-5.

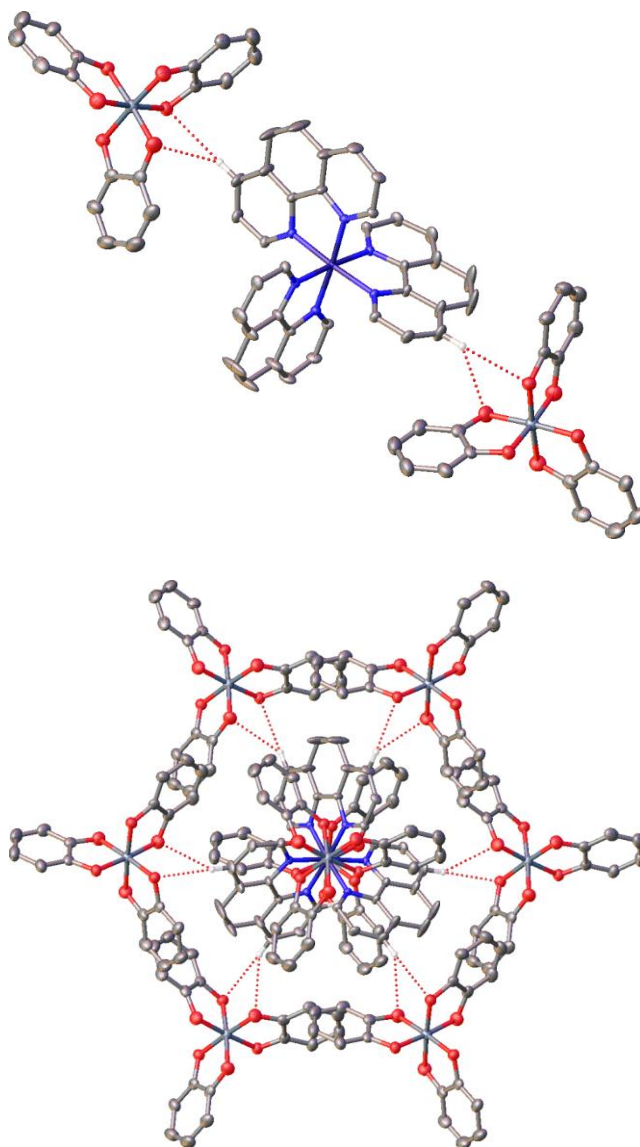


Figure S11. (top) Lateral interactions between Δ -TRISCAS and Λ -Fe(II) complexes in **3**. (bottom) Formation of Δ TRISCAS anionic shell around the triad structure in complex **3** as seen along the crystallographic c axis.

Weaker interactions mediated by hydrogen bonds are seen with other anions which are close to the Fe-N bonds direction (Figure 3), with $d_{\text{Fe-P}} = 9.1750(4)$ Å and $d_{\text{Fe-As}} = 9.1932(11)$ Å for complexes **2** and **3** respectively. Therefore, each complex is surrounded by six anions, forming a shell along the crystallographic c axis. The average distance between two phosphorus (arsenic) atoms in this shell is 9.2 Å (10.4 Å).

The dichloromethane molecules fill the void spaces between the triads. The average contacts and distances between cations and anions for complexes **2-5** are very similar (Table S10). We observe heterochiral interactions within the triads, mediated mainly through hydrogen bonding between the α -acidic hydrogens of the phenanthroline ligand and the oxygen atoms of the anion ($\text{C-H}\cdots\text{O} \approx 3.3$ Å) and some aromatic carbons ($\text{C-H}\cdots\text{C}(\pi) \approx 3.5\text{-}3.7$ Å), completed by a strong oxygen-carbon π - π interaction ($\text{O}(\pi)\cdots\text{C}(\pi) \approx 3.1\text{-}3.2$ Å).

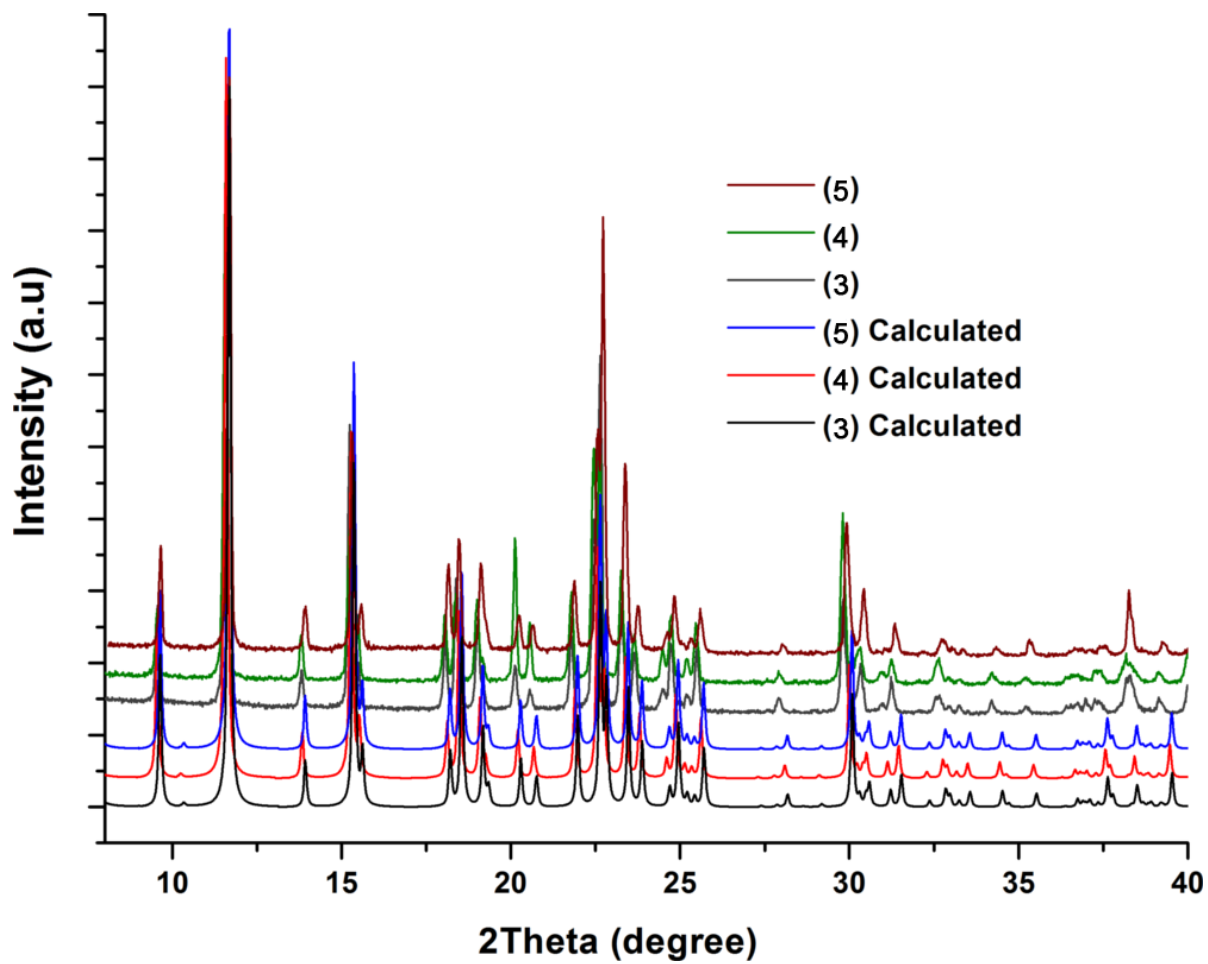


Figure S12. Powder diffractograms of complexes 3, 4 and 5 and corresponding powder diffraction patterns calculated from the X-ray structure.

Complex	Complex 4b	Complex 5b	Complex 4c	Complex 5c
	$[\Delta\text{-Fe(phen)}_3](\Lambda\text{-TRISCAS})_2$	$[\Lambda\text{-Fe(phen)}_3](\Lambda\text{-TRISCAS})_2$	$[\Delta\text{-Fe(phen)}_3](\Lambda\text{-TRISCAS})_2$	$[\Lambda\text{-Fe(phen)}_3](\Lambda\text{-TRISCAS})_2$
Formula	$\text{C}_{74}\text{H}_{48}\text{As}_2\text{FeN}_7\text{O}_{12}$	$\text{C}_{74}\text{H}_{51}\text{As}_2\text{FeN}_7\text{O}_{12}$	$\text{C}_{74}\text{H}_{51}\text{As}_2\text{FeN}_7\text{O}_{12}$	$\text{C}_{74}\text{H}_{48}\text{As}_2\text{FeN}_7\text{O}_{12}$
Formula weight ($\text{g}\cdot\text{mol}^{-1}$)	1432.88	1435.91	1435.91	1432.88
Crystal color			Red	
Crystal size (mm)	0.16×0.12×0.08	0.1×0.1×0.06	0.1×0.06×0.02	0.04×0.04×0.04
<i>T</i> (K)	200(2)	120(2)	120(2)	120(2)
Wavelength (Å)			0.71073	
Crystal system			Trigonal	
Space group			<i>R</i> 32	
<i>a</i> (Å)	15.0584(14)	15.0122(18)	15.015(3)	15.021(2)
<i>c</i> (Å)	25.789(4)	25.676(5)	25.696(5)	25.691(5)
<i>V</i> (Å ³)	5064.3(12)	5011.2(13)	5017.1(16)	5020.0(14)
<i>Z</i>			3	
ρ_{calc} ($\text{g}\cdot\text{cm}^{-3}$)	1.409	1.427	1.426	1.422
μ (mm^{-1})	1.264	1.278	1.276	1.275
<i>F</i> (000)	2187	2196	2196.0	2187.0
θ range (°)	2.705 ≤ θ ≤ 27.498	1.756 ≤ θ ≤ 27.566	1.755 ≤ θ ≤ 27.507	1.755 ≤ θ ≤ 27.499
Index ranges	-19 ≤ <i>h</i> ≤ 19 -19 ≤ <i>k</i> ≤ 19 -33 ≤ <i>l</i> ≤ 33	-19 ≤ <i>h</i> ≤ 19 -18 ≤ <i>k</i> ≤ 19 -33 ≤ <i>l</i> ≤ 33	-19 ≤ <i>h</i> ≤ 19 -19 ≤ <i>k</i> ≤ 19 -33 ≤ <i>l</i> ≤ 33	-19 ≤ <i>h</i> ≤ 19 -19 ≤ <i>k</i> ≤ 19 -33 ≤ <i>l</i> ≤ 33
Total refls.	44387	28522	48802	40112
Absorption correction			Sadabs	
<i>T</i> _{min} , <i>T</i> _{max}	0.7161, 0.7456	0.6691, 0.7456	0.6926, 0.7456	0.6667, 0.7456
Unique refls. (<i>I</i> > 2σ(<i>I</i>))	2474	2399	2311	2186
Completeness (θ=25.19°, %)	0.998	0.999	0.999	0.999
<i>R</i> _{int}	0.0279	0.0337	0.0581	0.0753
Refined param./restr.	150/0	151/0	151/0	150/0
Final <i>R</i> indices (<i>I</i> > 2σ(<i>I</i>))	<i>R</i> 1=0.0236 w <i>R</i> 2=0.0628	<i>R</i> 1=0.0237 w <i>R</i> 2=0.0627	<i>R</i> 1=0.0273 w <i>R</i> 2=0.0656	<i>R</i> 1=0.0318 w <i>R</i> 2=0.0696
<i>R</i> indices (all data)	<i>R</i> 1=0.0219 w <i>R</i> 2=0.0637	<i>R</i> 1=0.0274 w <i>R</i> 2=0.0644	<i>R</i> 1=0.0348 w <i>R</i> 2=0.0685	<i>R</i> 1=0.0459 w <i>R</i> 2=0.0739
Goodness-of-fit on <i>F</i> ²	1.118	1.079	1.082	1.067
(Δ / σ) _{max}	0.001	0.001	0	0
Δρ _{max} / Δρ _{min} (e ⁻ Å ⁻³)	0.313/-0.314	0.477/-0.301	0.463/-0.287	0.53/-0.414
Flack parameter	0.060(2)	0.003(4)	0.005(4)	-0.006(6)
Friedel coverage			1	

Table S13. Crystallographic data for complexes **4b**, **5b**, **4c**, **5c**.

As can be readily seen, the structures **4b-c** and **5b-c** are totally isomorphous with **4** and **5**. Enantiopurity is supported by the Flack parameter values of 0.060(2) (**4b**), 0.003(4) (**5b**), 0.005(4) (**4c**), -0.006(6) (**5c**). While $[\text{Fe}(\text{phen})_3](\text{TRISCAS})_2$ triads and the TRISCAS anionic shells are preserved, acetonitrile molecules replace dichloromethane in the void spaces. The heterochiral interaction is conserved as well between cationic complexes and TRISCAS anions within the triad and in the surrounding shell.

Synthesis of complexes 6-9

[Fe(phen)₃](rac-TRISPHAT)₂ (6). Crystals can be obtained in a few days by layering over a freshly prepared solution of 1,10-phenanthroline (54 mg, 0.3 mmol) and TRISPHAT.HNBu₃ (191 mg, 0.2 mmol) in 1 mL/3 mL MeCN/CH₂Cl₂, first a 2 mL 1:1 mixture of CH₂Cl₂/MeOH, then a solution of Fe(H₂O)₇.SO₄ (28 mg, 0.1 mmol) in 4 mL MeOH in a Schlenck tube under nitrogen. Two different crystal morphologies were observed, hard deep red prisms and small crumbly light red-orange sheets. The latter proved to be too sensitive to be measured, even when protective oil was used, very likely because they are too solvated.

Structure determination of the red prisms showed the expected structure, with the asymmetric unit in the monoclinic cell containing half a Fe(II) cation, with the Fe atom lying on the crystallographic twofold axis, and one whole phosphate counter anion in general position.

Out of the residual electronic density difference map only one disordered dichloromethane molecule could be identified, with the C-Cl bond lying on a crystallographic 2 axis, but no satisfactory discrete model could be achieved. So the SQUEEZE procedure²² as implemented in WinGX/PLATON²³ was applied starting with an asymmetric unit containing only the Fe(II) cation and the phosphate anion. The calculated electronic density (687 e⁻) could correspond to 16 dichloromethane solvent molecules (656 e⁻) in the unit cell. The corresponding solvent accessible volumes (2852 Å³, 29.1% of the unit cell) could nevertheless accommodate as much as four times as many dichloromethane molecules, so it is likely that the solvent content of those crystals is higher (and easily modified, as evidenced by the elemental analysis on bulk material where all solvent has been naturally replaced by water).

The aspect of the crystallization Schlenck tube did not change after a few weeks standing. But when the same tube was warmed at 55 °C, the orange product disappeared overnight. X-ray diffraction of the red powder obtained showed a different diffractogram from one simulated from the structure of solvated **6**.

²² SQUEEZE: P. van der Sluis, A. L. Spek *Acta Crystallogr. A*, **1990**, *46*, 194. A. L. Spek *Acta Crystallogr. C*, **2015**, *71*, 9.

²³ PLATON: A. L. Spek *J. Appl. Cryst.*, **2003**, *36*, 7.

[Fe(phen)₃][Δ-As₂(tartrate)₂] (7). A freshly prepared solution of (NBu₄)₂[Δ-As₂(tartrate)₂] (167 mg, 0.18 mmol) dissolved in 4 mL of a 1:1 mixture of CH₂Cl₂/MeOH in a Schlenk tube under argon was layered first with 5 mL of a 1:1 mixture of CH₂Cl₂/MeOH, then with a solution of Fe(H₂O)₇(SO₄) (50 mg, 0.18 mmol) and 1,10-phenanthroline (97 mg, 0.54 mmol) in 2.5 mL of MeOH. After two weeks, dark red powder and needle single crystals were obtained, then filtered and washed with cold methanol. Yield : 158 mg (73%) . Elemental Anal. Calcd. (%) for C₄₄H₂₈As₂FeN₆O₁₂(H₂O)_{8.7} (1195.15 g/mol): As 12.54; Fe 4.68; C 44.22; H 3.83; N 7.03. Found (%): As 12.11; Fe 5.13; C 44.30; H 3.80; N 6.94. IR (ATR, cm⁻¹): 3088w, 3021w [ν(C–H) aromatic]; 2914w [ν(C–H) alkane]; 1636s, 1633s, [br, ν(C=N)imine; ν(C=O)]; 1604m; 1579w, 1511w, 1494w, 1457w [ν(C=C)aromatic]; 1427m, 1413w, 1357m, 1340m, 1329m, 1228w, 1213w, 1143w, 1129m [δ(C–H)]; 1096w, 1075w, 1056w [ν(C–O)]; 848s, 843s [ν(As–O)]; 926w, 902w, 813w, 800w, 775w, 734m, 722s, 660m, 635m [δ (=C–H), δ(C–H)].

Structure determination of the needles showed an asymmetric unit containing one half cation and anion lying on crystallographic twofold axes. Out of the residual electronic density difference map only at least two dichloromethane molecules could be identified in general positions lying close to one threefold screw axis. Another solvent molecule could be seen lying on the same twofold axis than the cationic complex and very close to it, but could not be identified unambiguously as either dichloromethane or methanol. Overall no acceptable discrete model could be achieved for the solvent molecules, likely due to both strong steric hindrance and some diffuse character: indeed when considering only anions and cations, the remaining solvent-accessible space is contiguous and helicoidally shaped along the threefold screw axes shared by neighbouring unit cells. The corresponding electronic density was determined, then masked to refine the structure following the procedure available in Olex2.²⁴ The calculated electronic density correspond to 3 MeOH and between 6 and 12 dichloromethane solvent molecules (between 306 and 558 e⁻) in the unit cell. It must be noted that the calculated solvent-accessible volume is similar for all three complexes (between 734.5 and 771.1 Å³), and corresponds rather to the (MeOH)₃(CH₂Cl₂)₁₂ formulation (yielding 18 Å³ per solvent heavy atom on average).

²⁴ B. Rees, L. Jenner, M Yusupov *Acta Cryst. D*, **2005**, *61*, 1299.

[Fe(phen)₃][Λ-As₂(tartrate)₂] (8). A freshly prepared solution of 1,10-phenanthroline (97 mg, 0.54 mmol) and (NBu₄)₂[Λ-As₂(tartrate)₂] (167 mg, 0.18 mmol) dissolved in 4 mL of a 1:1 mixture of CH₂Cl₂/MeOH in a Schlenck tube under argon, was layered first with 5 mL of a 1:1 mixture of CH₂Cl₂/MeOH then with a solution of Fe(H₂O)₇(SO₄) (50 mg, 0.18 mmol) in 2.5 mL MeOH. After 3 weeks, red single crystal needles were obtained, then filtered and washed with cold methanol. Yield : 140 mg (62%). Elemental Anal. Calcd. (%) for C₄₄H₂₈As₂FeN₆O₁₂(CH₂Cl₂)_{1.6}(H₂O)₅ (1264.38g/mol): As 11.85; Fe 4.41; C 43.31; H 3.28 ; N 6.64. Found (%): As 11.64; Fe 5.02; C 43.27; H 3.20; N 6.68. IR (ATR, cm⁻¹): 3090w, 3019w [ν(C–H) aromatic]; 2915w [ν(C–H) alkane]; 1635s [br, ν(C=N)imine; ν(C=O)]; 1603m; 1579w, 1521w, 1517w, 1507w, 1457w [ν(C=C)aromatic]; 1427m, 1413w, 1356m, 1340m, 1330w, 1280w, 1228w, 1213w, , 1129w, 1143w, 1128w [δ(C–H)]; 1095w, 1075w, 1056w [ν(C–O)]; 848s, 844s [ν(As–O)]; 926w, 901w, 813m, 800w, 775w, 734m, 721s, 661m, 634m [δ (=C–H), δ(C–H)].

[Fe(phen)₃][As₂(tartrate)₂] (9). A freshly prepared solution of an equimolar mixture of [Δ/Λ-As₂(tartrate)₂](NBu₄)₂ (167 mg, 0.18 mmol) dissolved in 4 mL of a 1:1 mixture of CH₂Cl₂/MeOH in a Schlenck tube under argon was layered first with 5 mL of a 1:1 mixture of CH₂Cl₂/MeOH, then with a solution of Fe(H₂O)₇(SO₄) (50 mg, 0.18 mmol) and 1,10-phenanthroline (97 mg, 0.54 mmol) in 2.5 mL of MeOH. After two weeks, dark red powder and needle single crystals were obtained, filtered and washed with cold methanol. Yield : 155 mg (72%) . Elemental Anal. Calcd. (%) for C₄₄H₂₈As₂FeN₆O₁₂(CH₂Cl₂)(H₂O)₅ (1213.42 g/mol): As 12.35; Fe 4.60; C 44.54; H 3.32; N 6.93. Found (%): As 11.86; Fe 4.65; C 44.61; H 3.58; N 7.09. IR (ATR, cm⁻¹): 3088w, 3020w [ν(C–H)aromatic]; 2915w [ν(C–H) alkane]; 1637s, 1632s, [br, ν(C=N)imine, ν(C=O)]; 1602m; 1577w, 1559w, 1507w, 1458w [ν(C=C)aromatic]; 1427m, 1413w, 1356w, 1340m, 1329m, 1227w, 1214w, 1142w, 1128m, [δ(C–H)]; 1095w, 1075w, 1055w [ν(C–O)]; 847s, 843s [ν(As–O)]; 926w, 901w, 813w, 800w, 775w, 735m, 721s, 660m, 634m [δ (=C–H), δ(C–H)].

Crystallographic data for complexes 6-9

Complex	Complex 6
	[rac-Fe(phen) ₃](rac-TRISPHAT) ₂
Formula	C ₇₆ H ₃₂ Cl ₃₂ FeN ₆ O ₁₂ P ₂
Formula weight (g·mol ⁻¹)	2473.38
Crystal color	red
Crystal size (mm)	0.28×0.2×0.2
<i>T</i> (K)	120(2)
Wavelength (Å)	0.71073
Crystal system	monoclinic
Space group	C2/c
<i>a</i> (Å)	25.435(2)
<i>b</i> (Å)	17.1762(15)
<i>c</i> (Å)	23.786(2)
β (°)	109.202(2)
<i>V</i> (Å ³)	9813.4(14)
<i>Z</i>	4
ρ_{calc} (g·cm ⁻³)	1.674
μ (mm ⁻¹)	1.117
<i>F</i> (000)	4904
θ range (°)	1.86 ≤ θ ≤ 30.04
	-35 ≤ <i>h</i> ≤ 32
Index ranges	-22 ≤ <i>k</i> ≤ 24
	-25 ≤ <i>l</i> ≤ 33
Total refls.	37927
Absorption correction	scalepack
<i>T</i> _{min} , <i>T</i> _{max}	0.745, 0.8075
Unique refls. (<i>I</i> > 2σ(<i>I</i>))	10939
Completeness (θ=25.19°, %)	0.995
<i>R</i> _{int}	0.0319
Refined param./restr.	528/0
Final <i>R</i> indices (<i>I</i> > 2σ(<i>I</i>))	<i>R</i> 1=0.0438
	w <i>R</i> 2=0.1309
	<i>R</i> 1=0.0575
	w <i>R</i> 2=0.1382
Goodness-of-fit on <i>F</i> ²	1.033
(Δ / σ) _{max}	0.002
Δρ _{max} / Δρ _{min} (e ⁻ Å ⁻³)	0.624 / -0.588

Table S14. Crystallographic data for complex 6.

Complex	Complex 7	Complex 8	Complex 9
	[Δ -Fe(<i>phen</i>) ₃][Δ -As ₂ (tartrate) ₂]	[Λ -Fe(<i>phen</i>) ₃][Λ -As ₂ (tartrate) ₂]	[rac-Fe(<i>phen</i>) ₃][rac-As ₂ (tartrate) ₂]
Formula		C ₄₄ H ₂₈ As ₂ FeN ₆ O ₁₂	
Formula weight (g·mol ⁻¹)		1038.41	
Crystal color	dark red	light red	dark red
Crystal size (mm)	0.24×0.22×0.22	0.24×0.04×0.04	0.34×0.18×0.18
<i>T</i> (K)		120(2)	
Wavelength (Å)		0.71073	
Crystal system		Trigonal	
Space group	<i>P</i> 3 ₁ 21	<i>P</i> 3 ₂ 21	<i>P</i> 3 ₁ 21
<i>a</i> (Å)	18.3549(19)	18.324(6)	18.415(3)
<i>c</i> (Å)	11.8899(12)	11.894(4)	11.8794(16)
<i>V</i> (Å ³)	3469.1(8)	3459(2)	3488.8(11)
<i>Z</i>		3	
ρ_{calc} (g·cm ⁻³)	1.491	1.496	1.483
μ (mm ⁻¹)	1.813	1.818	1.802
F(000)		1566.0	
θ range (°)	2.139 ≤ θ ≤ 27.492	1.283 ≤ θ ≤ 27.497	1.277 ≤ θ ≤ 27.488
Index ranges	-23 ≤ <i>h</i> ≤ 23 -23 ≤ <i>k</i> ≤ 23 -15 ≤ <i>l</i> ≤ 15	-21 ≤ <i>h</i> ≤ 23 -23 ≤ <i>k</i> ≤ 22 -15 ≤ <i>l</i> ≤ 15	-23 ≤ <i>h</i> ≤ 23 -23 ≤ <i>k</i> ≤ 23 -15 ≤ <i>l</i> ≤ 15
Total refls.	102505	34986	92895
Absorption correction		Sadabs	
<i>T</i> _{min} , <i>T</i> _{max}	0.7022, 0.7456	0.6219, 0.7456	0.6605, 0.7456
Unique refls. (<i>I</i> > 2 σ (<i>I</i>))	5217	3777	5244
Completeness (θ =25.19°, %)	0.998	0.995	0.997
<i>R</i> _{int}	0.0242	0.0849	0.0245
Refined param./restr.	294/0	294/0	295 /0
Final <i>R</i> indices (<i>I</i> > 2 σ (<i>I</i>))	<i>R</i> 1=0.0332 w <i>R</i> 2=0.0834	<i>R</i> 1=0.0541 w <i>R</i> 2=0.1188	<i>R</i> 1= 0.0346 w <i>R</i> 2= 0.0958
<i>R</i> indices (all data)	<i>R</i> 1=0.0338 w <i>R</i> 2=0.0837	<i>R</i> 1=0.0814 w <i>R</i> 2=0.128	<i>R</i> 1= 0.0354 w <i>R</i> 2= 0.0964
Goodness-of-fit on <i>F</i> ²	1.064	1.008	1.123
(Δ / σ) _{max}	0.001	0	0.001
$\Delta\rho_{\text{max}} / \Delta\rho_{\text{min}}$ (e ⁻ Å ⁻³)	0.474/-0.365	0.468/-0.442	0.51/-0.325
Flack parameter	0.021(4)	0.029(8)	0.492(13)
Friedel coverage	1	1	0.999

Table S15. Crystallographic data for complexes 7-9.

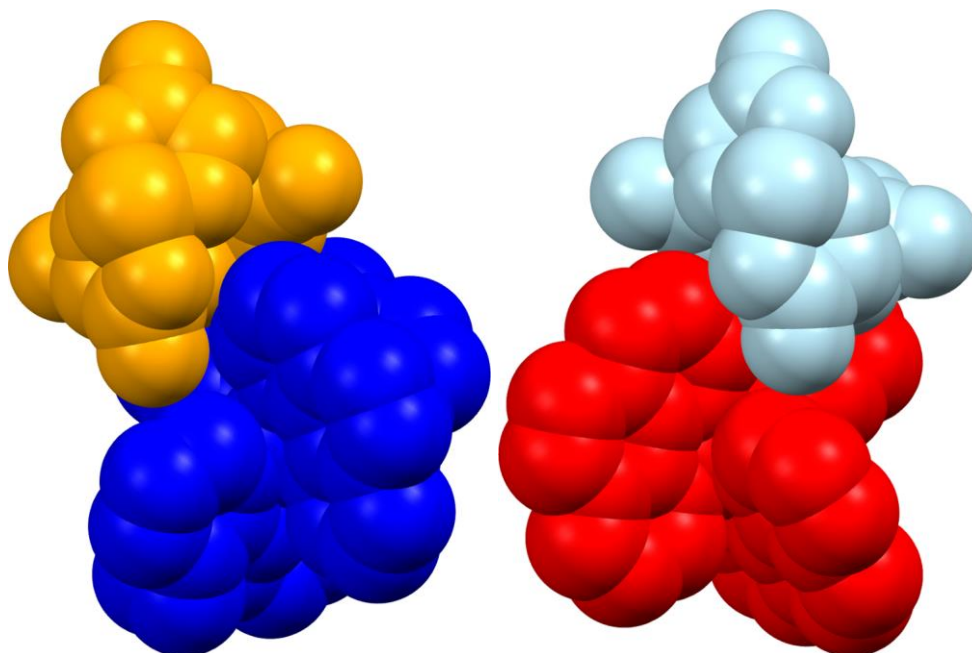


Figure S16. Van der Waals representation of homochiral interactions in complexes **7** and **8** between $[\text{Fe}(\text{phen})_3]^{2+}$ and $[\text{As}_2(\text{tartrate})_2]^{2-}$.

Left: $[\Delta\text{-Fe}(\text{phen})_3][\Delta\text{-As}_2(\text{tartrate})_2]$ (**7**) in blue and orange respectively. Right: $[\Lambda\text{-Fe}(\text{phen})_3][\Lambda\text{-As}_2(\text{tartrate})_2]$ (**8**) in red and light blue respectively.

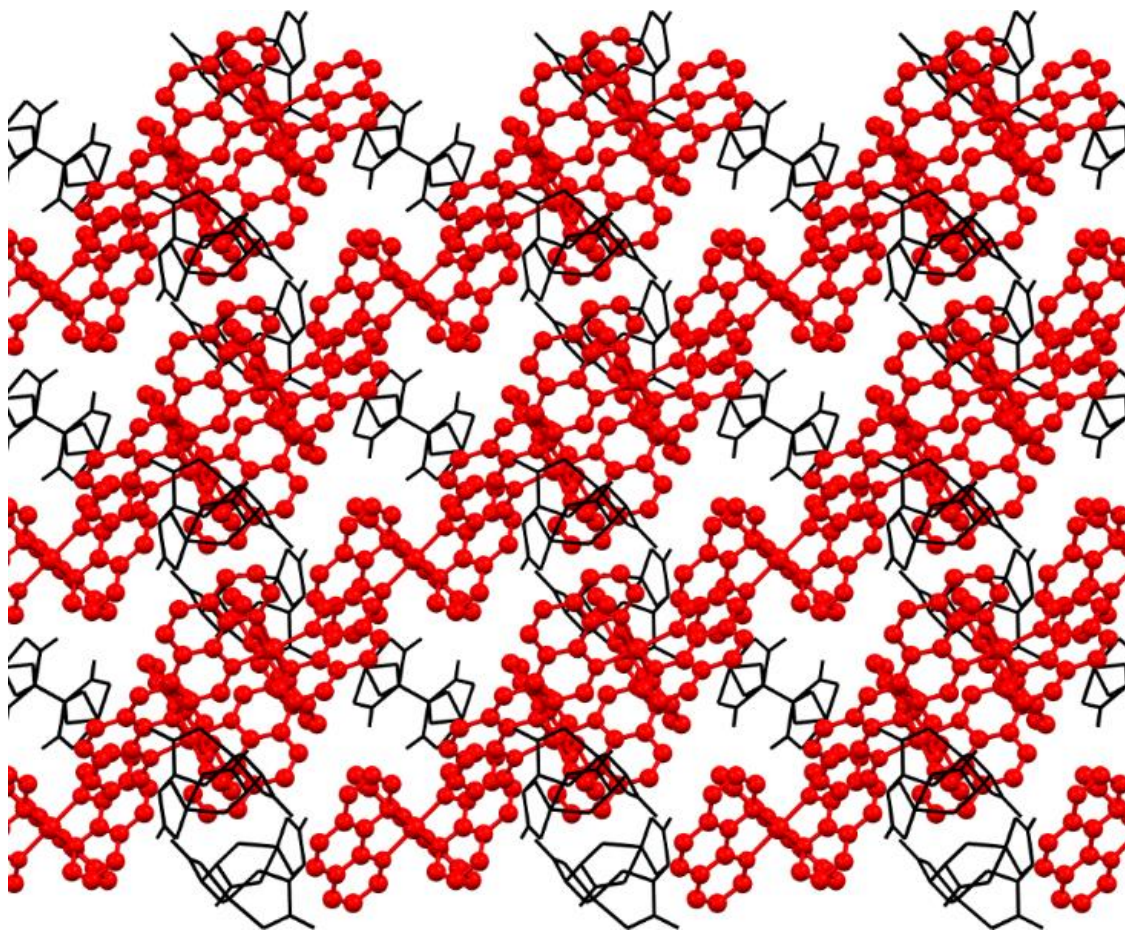


Figure S17. Crystal packing of complex **7** as seen along the *a* crystallographic axis. Cationic layers of $[\Lambda\text{-Fe}(\text{phen})_3]^{2+}$ are represented in red, counteranions are embedded within the positively charged layers shown in black.

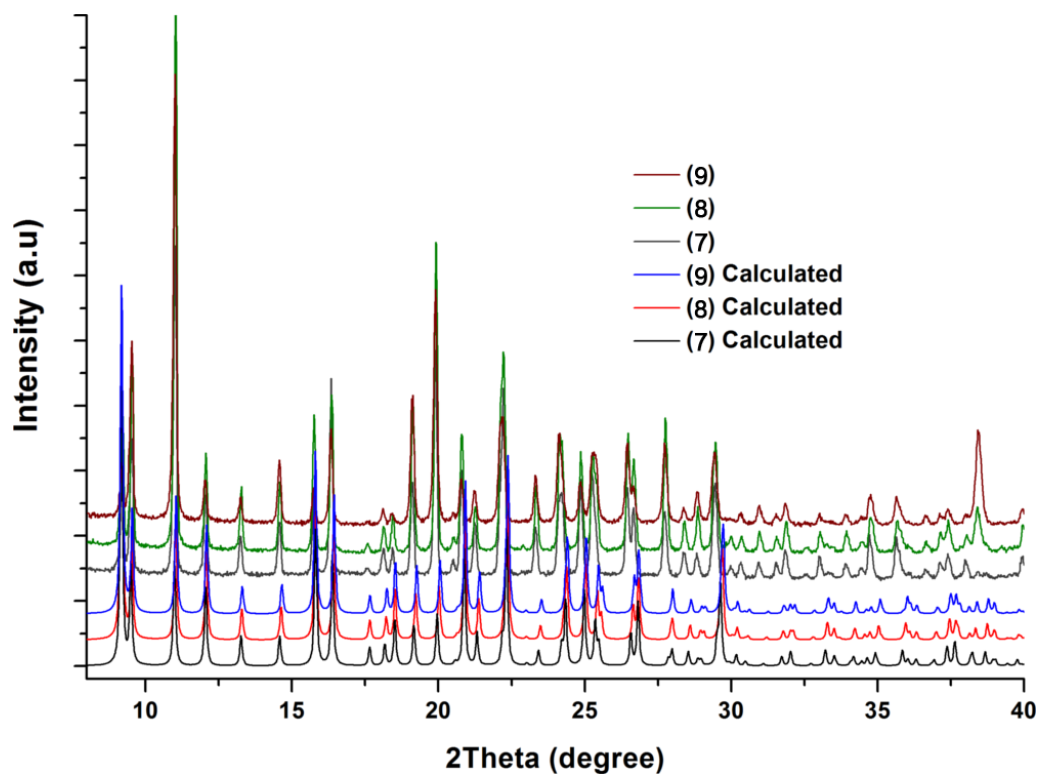


Figure S18. Comparison between bulk powder diffraction patterns (experimental) and calculated powder diffractograms for 7-9.

Spectroscopic data

Experimental details of CD and polarimeter measurements

CD experiments for solutions and KBr pellets were run on a Jasco J-815 spectrophotometer using a 2 mm path length cuvette or a special sample holder, respectively. KBr pellets were prepared by grinding a mixture of compound and oven-dried (130°C) KBr. The mixture was then pressed in a 13-mm die under good primary vacuum for 30min. All spectra shown here were measured with scan speed of 50 nm/min and a 2 nm bandwidth, with either high or normal amplifier gain. Background corrections were performed subtracting the spectrum obtained in the same measurement conditions either on a cuvette filled with pure solvent, or on a pellet prepared with pure KBr in the same conditions. CD data were converted to differential extinction coefficient ($\Delta\varepsilon$) based on concentration of the compounds using the following equation:²⁵

$$\Delta\varepsilon = \frac{\theta}{32980 \times c \times l}$$

where θ is the CD ellipticity in millidegrees, c is the concentration in mol.L⁻¹, and l is the path length in cm. The cl product was empirically determined for the pellets with the approximation that absorbance at the maximum of the band around 265 nm was considered equal for the pellet and for the solution transmission measurements. Neglecting all solid state effects on the electronic absorption spectrum is likely to be less important than all macroscopic anisotropic effects and the non-ideal characteristics of the spectrometer, which are known to make dichroic measurements in the solid state extremely difficult.²⁶

Specific rotations in solutions were measured on a Krüss Optronic P3002/RS automatic digital polarimeter (resolution : 0.001°) using a sodium bulb ($\lambda = 589$ nm) passing through a polarizing device and a modulator. Measurements were performed at $c = 0.01$ g.ml⁻¹.

²⁵ N. Berova, L. Di Bari, G. Pescitelli *Chem. Soc. Rev.*, **2007**, *36*, 914. A. Rodger, *Encyclopedia of Biophysics*, **2013**, 316.

²⁶ R. Kuroda in *Engineering of Crystalline Materials Properties*, J. J. Novoa et al Eds., Springer, *NATO Science for Peace and Security Series*, 2008, 251. R. Kuroda, T. Harada, in *Comprehensive Chiroptical Spectroscopy*, N. Berova et al. Eds, Wiley, **2012**, 91.

Specific optical rotations of chiral anions

<i>Anion</i>	<i>Solvent</i>	<i>Specific rotation</i> [α] _D ²⁵	<i>Diastereomeric excess (d.e)</i>
[Δ -TRISCAS cinchoninium]	acetone	-232.65°	88
		-228.02°	86
[Λ -TRISCAS cinchonidinium]		+175.78°	66
[Δ -As ₂ (tartrate) ₂](NBu ₄) ₂	acetonitrile	-33.2(5)	---
[Λ -As ₂ (tartrate) ₂](NBu ₄) ₂	acetonitrile	+34.0(10)	---
[Λ -Sb ₂ (tartrate) ₂]K ₂	water	+138.1(5)°	unknown (Sigma-Aldrich)

Absorption and CD spectra of $K_2[Sb_2(tartrate)_2]$ in water

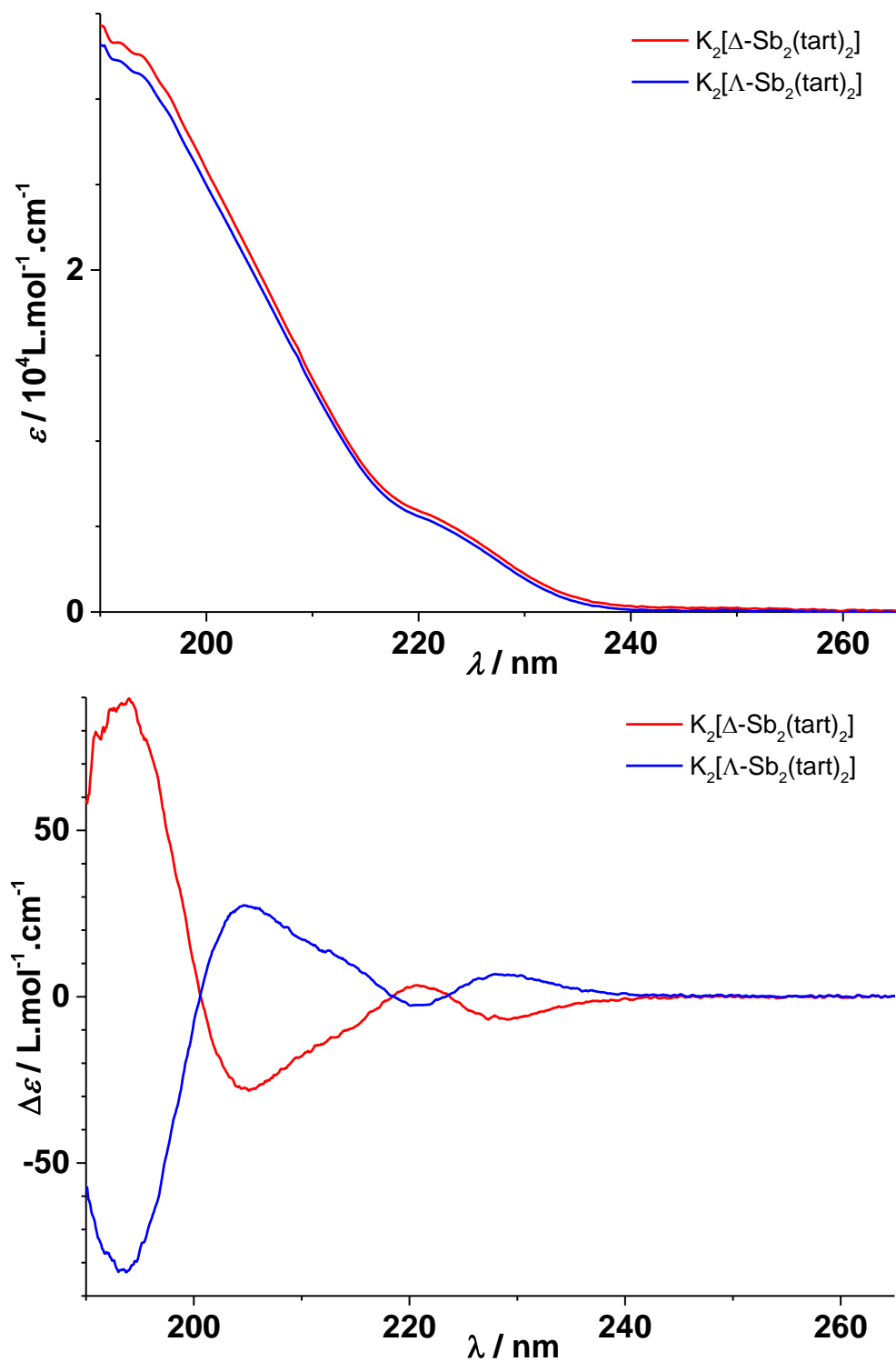


Figure S19. Electronic absorption (top) and CD (bottom) spectra of $K_2[\Delta\text{-Sb}_2(\text{tartrate})_2]$ (red line) and $K_2[\Lambda\text{-Sb}_2(\text{tartrate})_2]$ (blue line) in water between 190-265 nm.

Absorption and CD spectra of 1 in acetonitrile

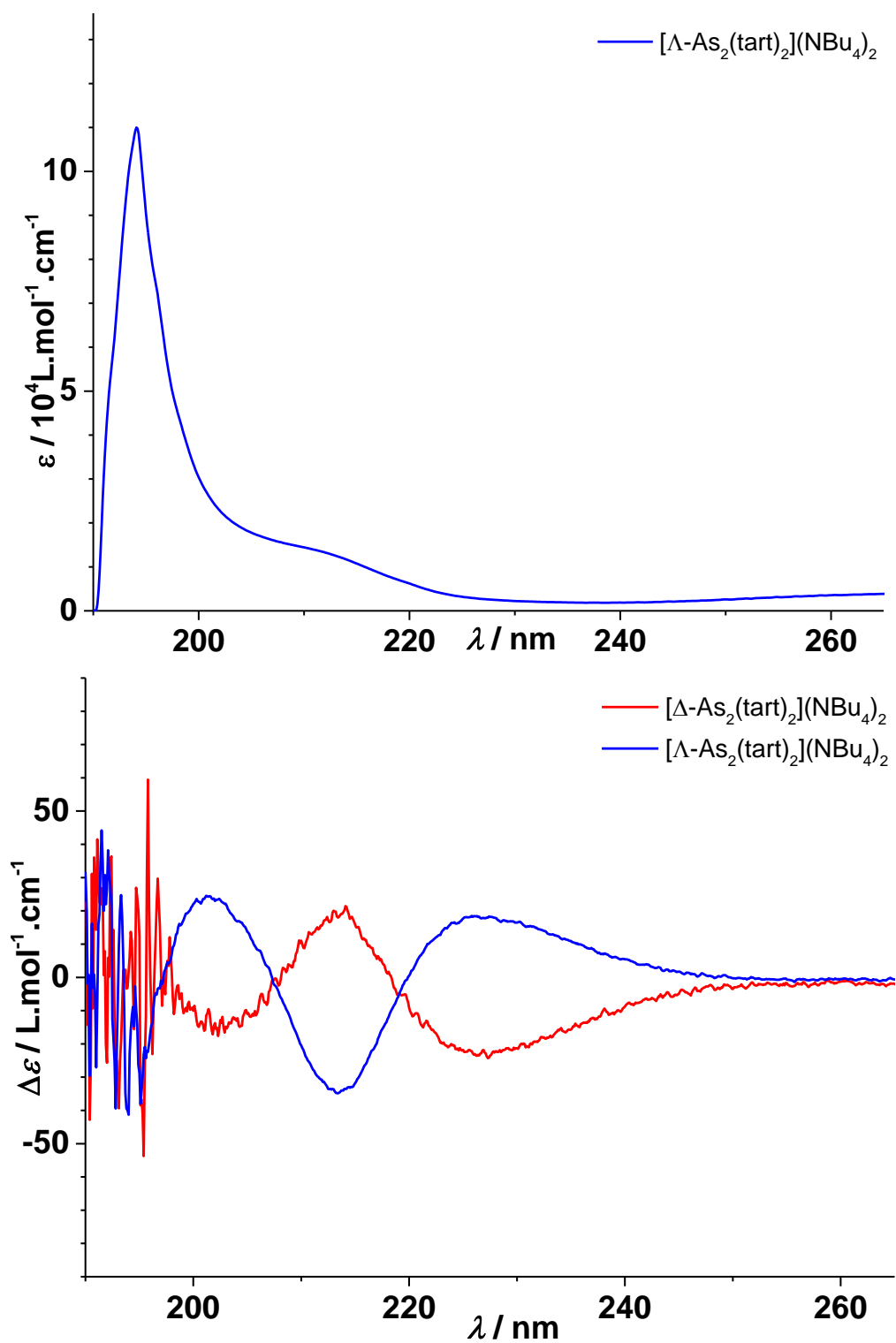


Figure S20. Electronic absorption (top) and CD (bottom) spectra of Δ -1 (red line) and Λ -1 (blue line) in MeCN between 190-265 nm.

CD spectra of **1** and (NBu₄)₂(tartrate) in water

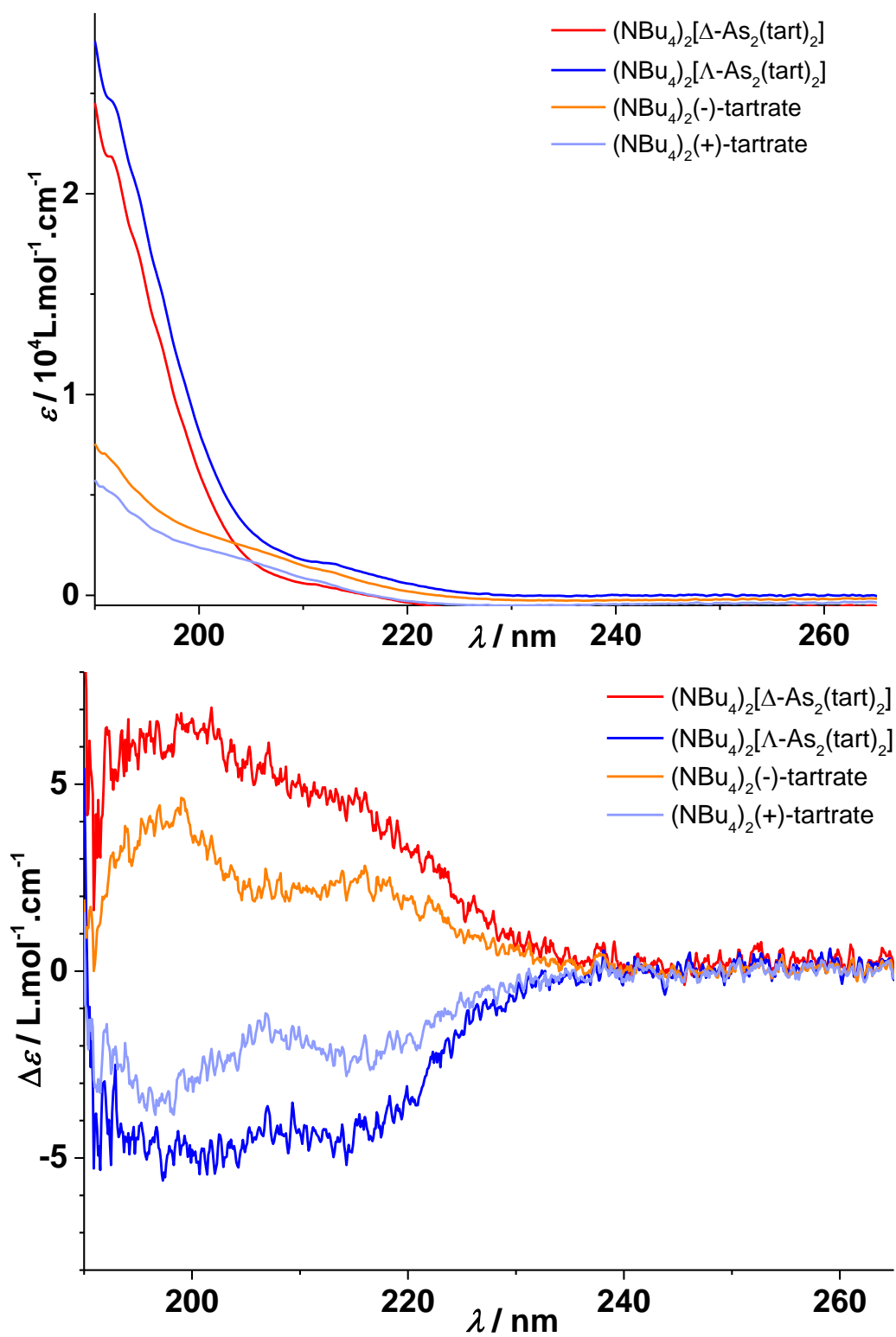


Figure S21. Comparison of UV-Vis and CD spectra of **1** and (NBu₄)₂(tartrate) in water between 190-265 nm.

Solid state CD spectra of **1**

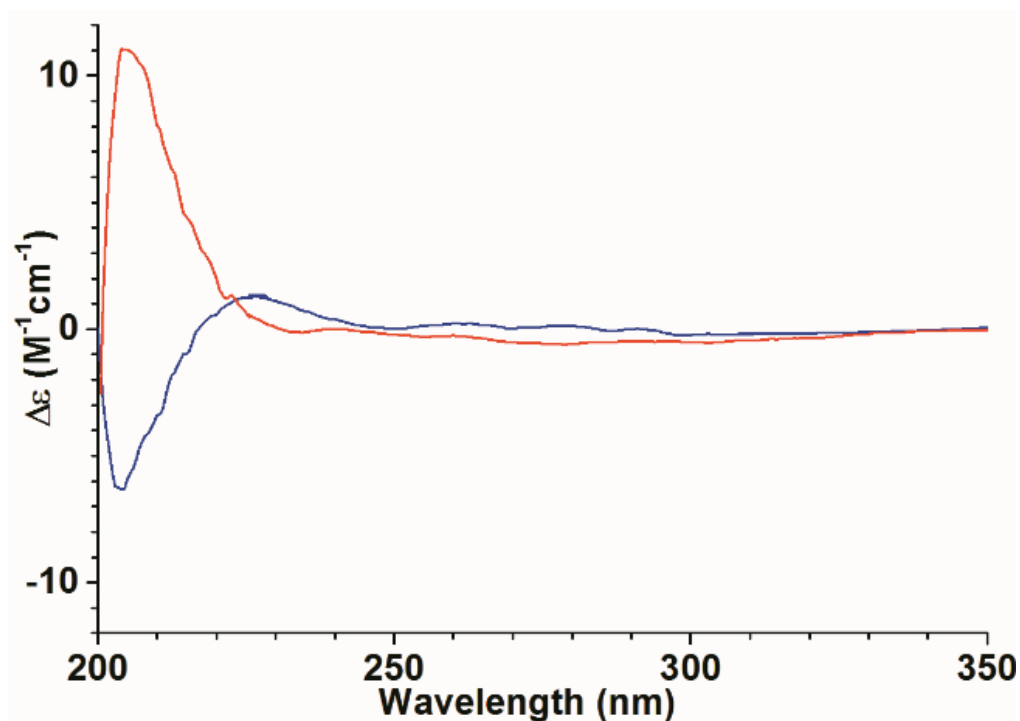


Figure S22. CD spectra of KBr pellets of Δ -**1** (red line) and Λ -**1** (blue line) between 200-350 nm.

For Λ -**1**, 120 mg of 3.95×10^{-4} w/w $(\text{NBu}_4)_2[\Lambda\text{-As}_2(\text{tartrate})_2]$ dispersed in oven-dried KBr was pressed under vacuum for 15 min in a $\text{Ø}13$ mm die into a 0.41 mm thick pellet. The resulting $lc=3.86 \times 10^{-5}$ cm·M product was used for CD calculations. For Δ -**1**, 120 mg of 3.73×10^{-4} w/w $(\text{NBu}_4)_2[\Delta\text{-As}_2(\text{tartrate})_2]$ dispersed in oven-dried KBr was pressed under vacuum for 15 min in a $\text{Ø}13$ mm die into a 0.41 mm thick pellet. The resulting $lc=3.67 \times 10^{-5}$ cm·M product was used for CD calculations. Baseline correction was checked using a pristine KBr pellet prepared in the same conditions.

Electronic spectra of complexes

UV-vis spectra $[\text{Fe}(\text{phen})_3](\text{X})_2$, X = TRISCAT (**2**), *rac*- (**3**), Δ - (**4**), Λ -TRISCAS (**5**), in acetonitrile: electronic absorption spectra were measured on an Agilent CARY-5000 spectrometer, using suprasil cuvettes with 1 cm path length, for solutions of complexes $[\text{Fe}(\text{phen})_3](\text{X})_2$ (X = TRISCAT **2** ($92 \mu\text{mol.L}^{-1}$), *rac*-TRISCAS **3** (0.1 mmol.L^{-1}), Δ -TRISCAS **4** ($44 \mu\text{mol.L}^{-1}$), Λ -TRISCAS **5** ($44 \mu\text{mol.L}^{-1}$)) and *rac*-TRISCAS)NBu₄ (0.11 mmol.L^{-1}) (Figure S23). The UV-visible spectra of **2-5** are very similar. A typical spectrum shows three intense MLCT bands involving Fe 3d orbitals and ligand π^* orbitals,²⁷ and they are overlapping each other in the 400-550 nm region forming a single broad band. In addition, below 350 nm, the π - π^* transitions of the ligand and the counter anions (TRISCAS, TRISCAT) are completely overlapping, with two sets of bands between 250 and 300 nm and below 240 nm. Molar extinction coefficients of the above complexes and the anion are shown in Table S24. It must be pointed out that the Fe spin-forbidden d-d transitions are very weak and lie around the same energy level as the MLCT bands.

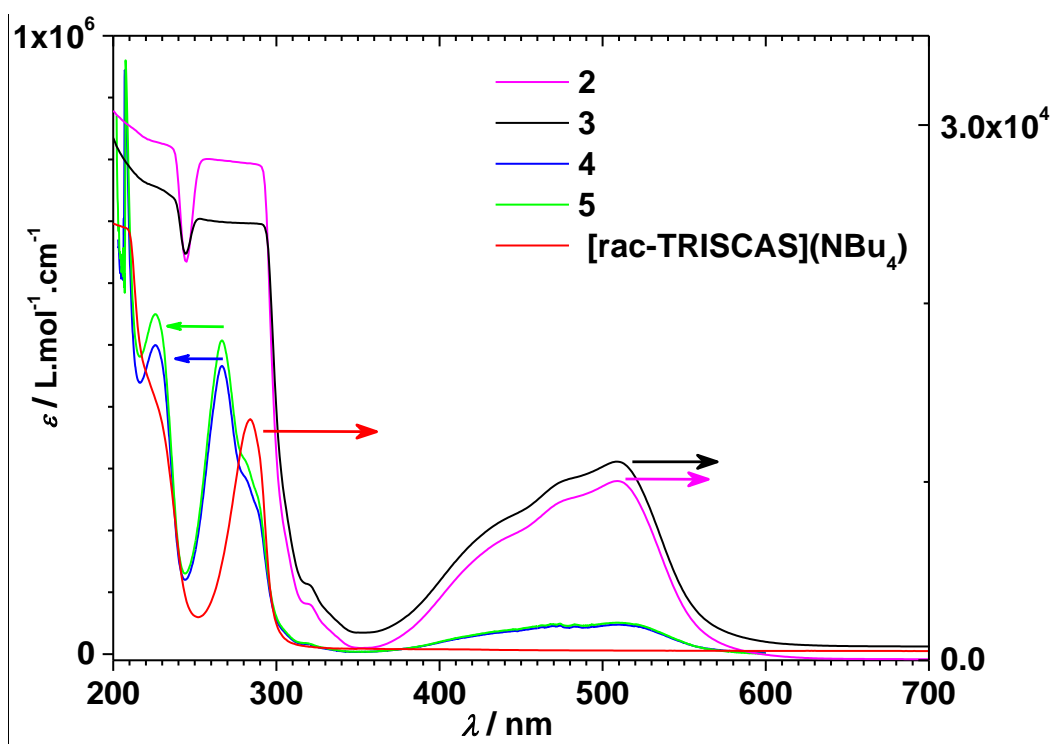


Figure S23. UV-vis spectra of **2** (magenta line), **3** (black line), **4** (blue line), **5** (green line), NBu₄(*rac*-TRISCAS) (red line) measured in acetonitrile at room temperature. Solutions of complexes **2** and **3** were concentrated (saturation below 350 nm).

²⁷ S. Savage, Z. Jia-Long, A. G. Maddock, *J. Chem. Soc., Dalton Trans.*, **1985**, 991.

Complex	Molar extinction coefficient ϵ ($10^3 \text{ L}\cdot\text{mol}^{-1}\cdot\text{cm}^{-1}$)			
	$\epsilon(284 \text{ nm})$	$\epsilon(430 \text{ nm})$	$\epsilon(470 \text{ nm})$	$\epsilon(510 \text{ nm})$
2	*	6.25	8.65	10
3	*	7.32	9.76	11.1
4	291	35.0	48.0	50.8
5	266	32.7	45.2	47.7
[rac-TRISCAS](NBu₄)	13.5	---	--	--

Table S24. Molar extinction coefficients for $[\text{Fe}(\text{phen})_3](\text{X})_2$, X = TRISCAT (**1**), rac-(**2**), Δ -(**3**), Λ -TRISCAS (**4**), measured in acetonitrile.

* solutions were too concentrated leading to saturation below 350 nm.

UV-vis spectra $[\text{Fe}(\text{phen})_3](\text{X})_2$, $\text{X} = \Delta^-$ (**7**), Δ^- -arsenyl tartrate (**8**) and racemic mixture (**9**), in acetonitrile: electronic absorption spectra were measured on solutions of $[\text{Fe}(\text{phen})_3](\Delta^- \text{As}_2(\text{tartrate})_2)$ **7** (0.1 mmol.L^{-1}), $[\text{Fe}(\text{phen})_3](\Delta^- \text{As}_2(\text{tartrate})_2)$ **8** (0.12 mmol.L^{-1}) and $[\text{Fe}(\text{phen})_3](\text{As}_2(\text{tartrate})_2)$ **9** ($89 \text{ } \mu\text{mol.L}^{-1}$) in acetonitrile.

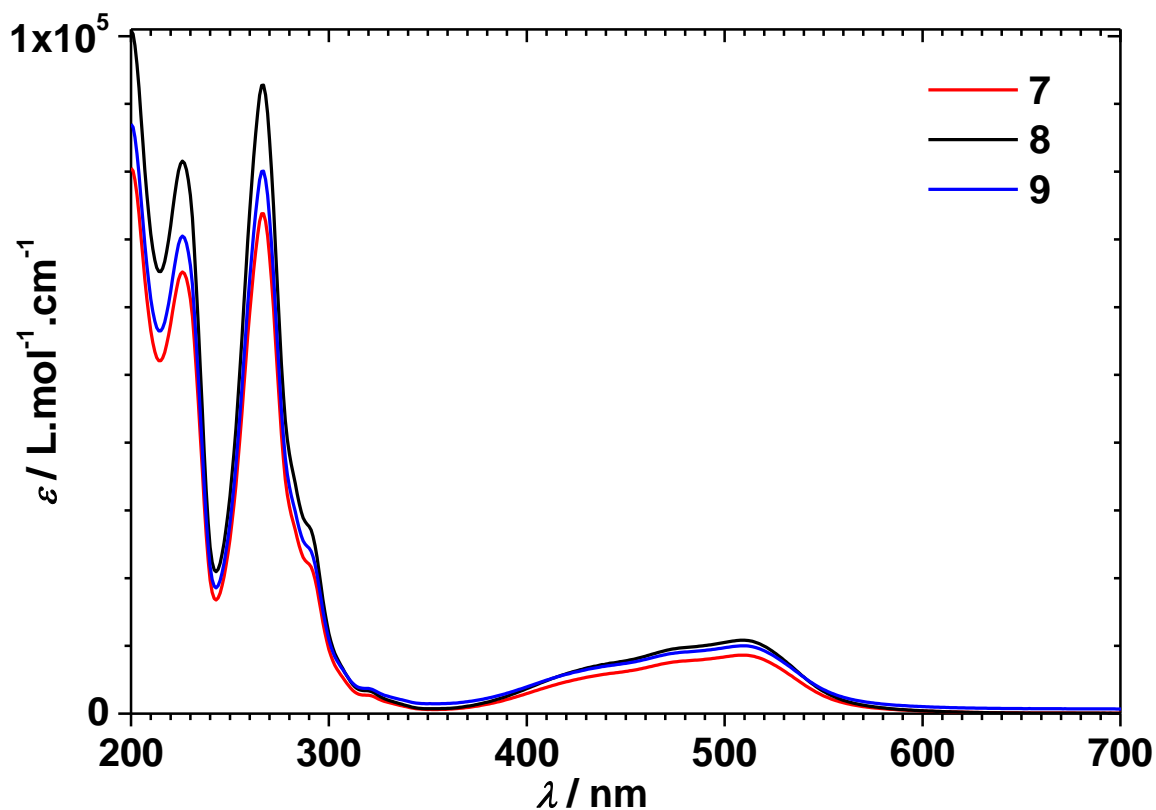


Figure S25. Electronic absorption spectra of complexes **7** (red line), **8** (black line), **9** (blue line) measured in acetonitrile at room temperature.

Molar extinction coefficients of complexes are shown in Table S26. Spectra of **7-9** show three overlapped MLCT bands at 510 nm, 470 nm and 430 nm, in the UV region below 350 nm, a small absorption band at 321 nm, a small shoulder at 290 nm overlapped with a strong intense absorption band at 266 nm and a second intense band at 226 nm. Bands at 226 nm and 321 nm can be assigned to the overlap of transitions in the tartaric acid moieties of the *D2*-chiral anion and transitions of the phenanthroline ligand,²⁸ while the lower energy UV bands at 290 nm and 266 nm can be assigned to π - π^* transitions of the phenanthroline ligand.

²⁸ a) J. Mason, S. F. Mason, *Tetrahedron*, **1967**, *23*, 1919. b) A. L. Brizard, D. Berthier, C. Aimé, T. Buffeteau, D. Cavagnat, L. Ducasse, I. Huc, R. Oda, *Chirality*, **2009**, *21*, 153. c) M. Hoffmann, J. Grajewski, J. Gawronski, *New J. Chem.*, **2010**, *34*, 2020.

λ (nm)	Complex ε (10^3 L.mol $^{-1}$ cm $^{-1}$)		
	7	8	9
510	10.8	10.0	8.68
470	9.25	8.65	7.35
430	6.64	6.62	5.27
321	3.22	3.59	2.62
290	27.4	24.2	22.0
266	92.6	79.8	73.7
226	81.3	70.3	65.1

Table S26. Molar extinction coefficients for [Fe(*phen*)₃](X)₂, X = Δ - (**7**), Λ -arsenyl tartrate (**8**) and racemic mixture (**9**), measured in acetonitrile.

Electronic and dichroic spectra of TRISCAS and alkaloid salts in acetonitrile

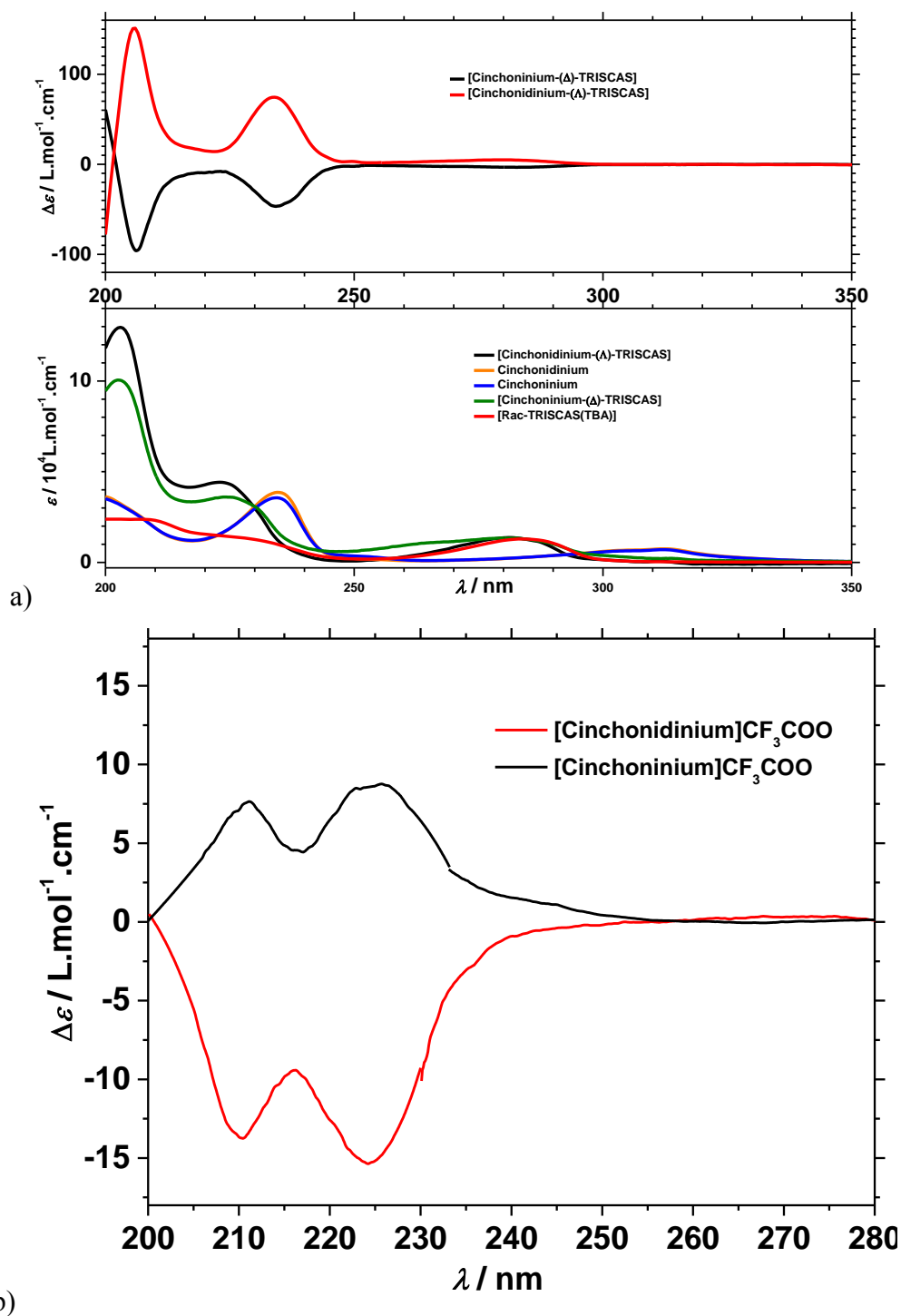


Figure S27. (a top) CD spectra of (Δ -TRISCAS)cinchoninium and (Λ -TRISCAS)cinchonidinium in acetonitrile solution; (a bottom) electronic spectra of (Δ -TRISCAS)cinchoninium, (Λ -TRISCAS)cinchonidinium, cinchoninium and cinchonidinium CF_3COO^- salts, and TRISCAS(NBu_4) in acetonitrile solution; (b) CD spectra of cinchoninium and cinchonidinium CF_3COO^- salts in acetonitrile solution.

NMR spectra

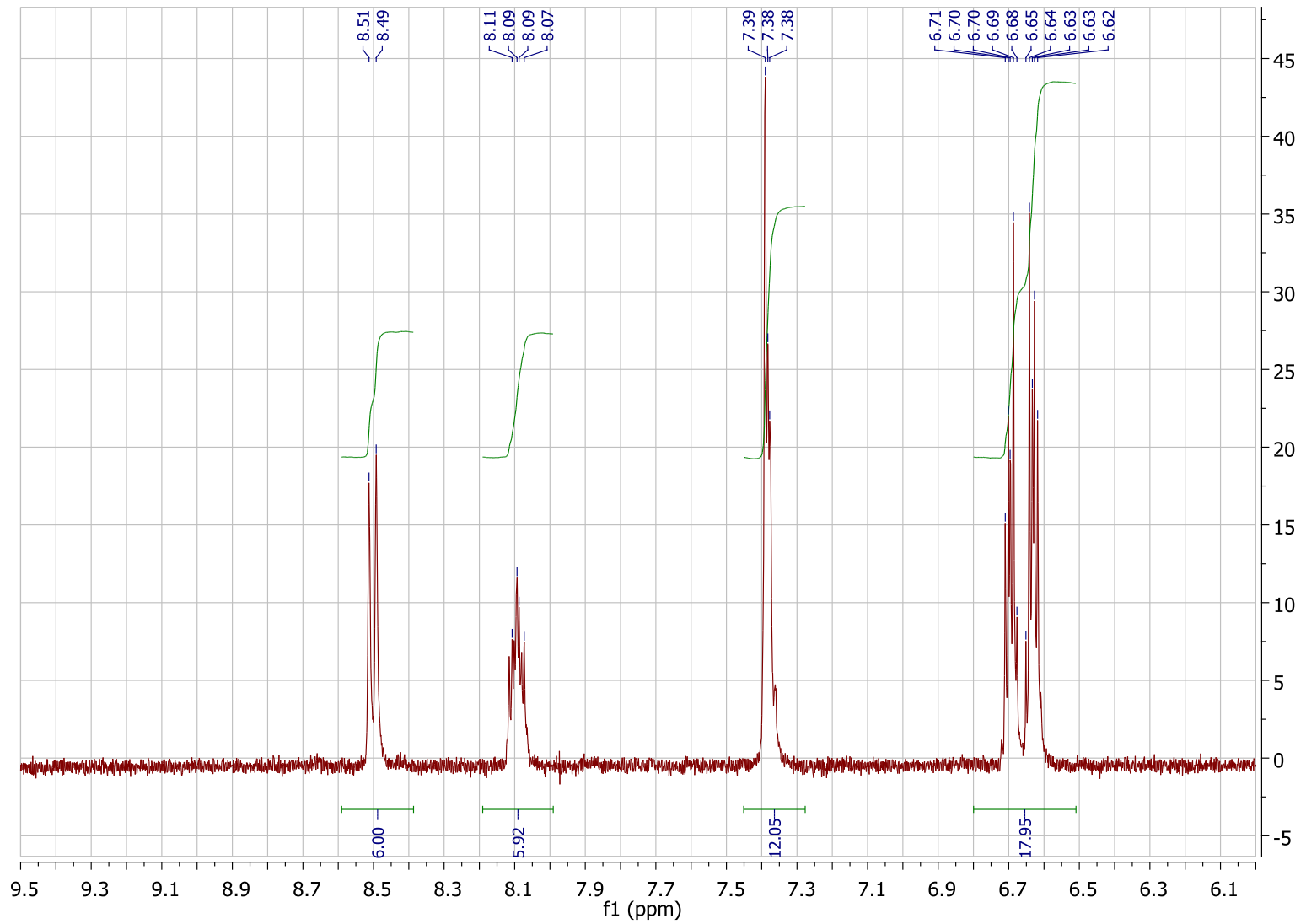


Figure S28a. NMR spectra of [Fe(phen)₃](rac-TRISCAS)₂ (3) in d₃-acetonitrile

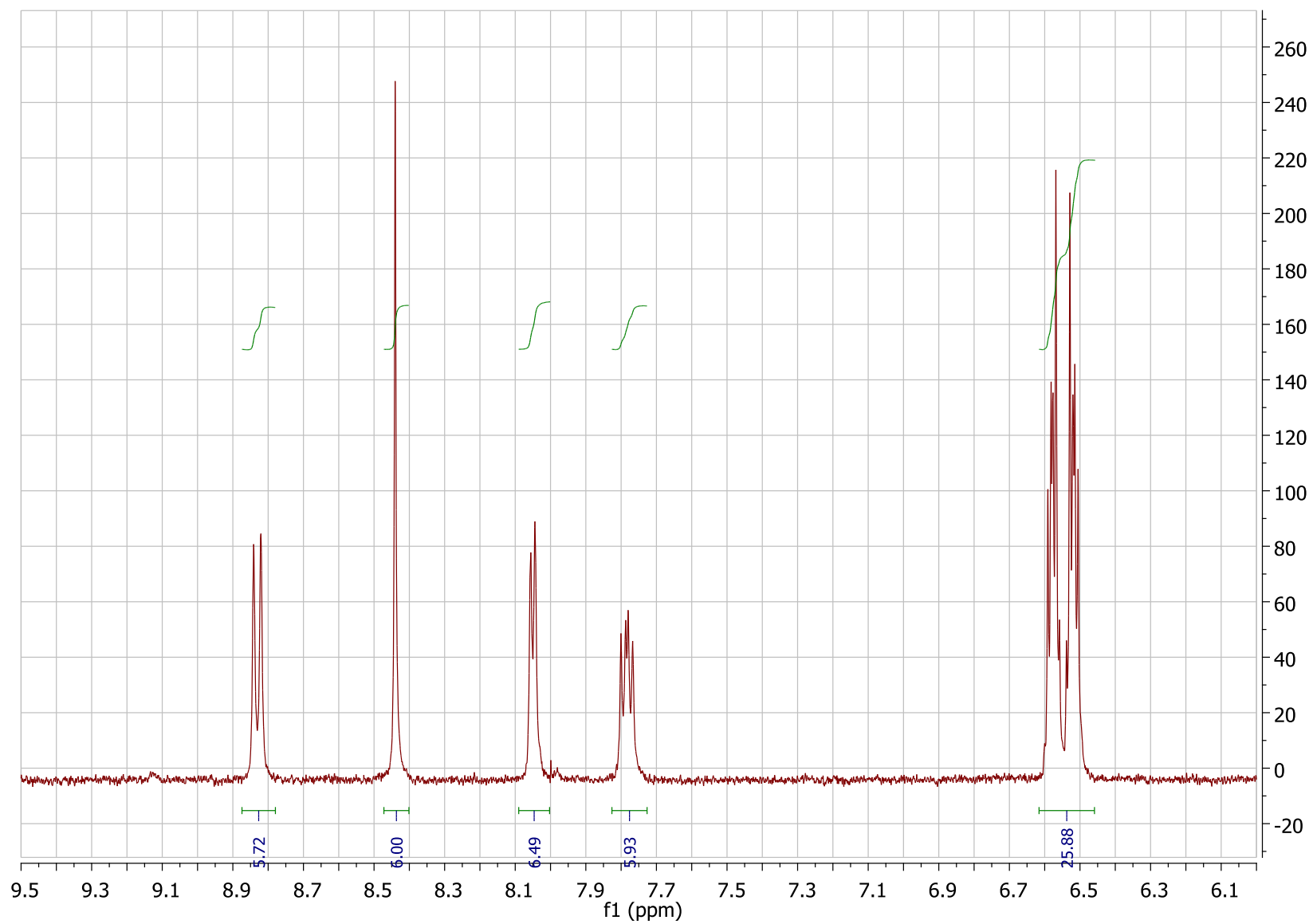


Figure S28b. NMR spectra of [Fe(phen)₃](rac-TRISCAS)₂ (3) in d₆-acetone

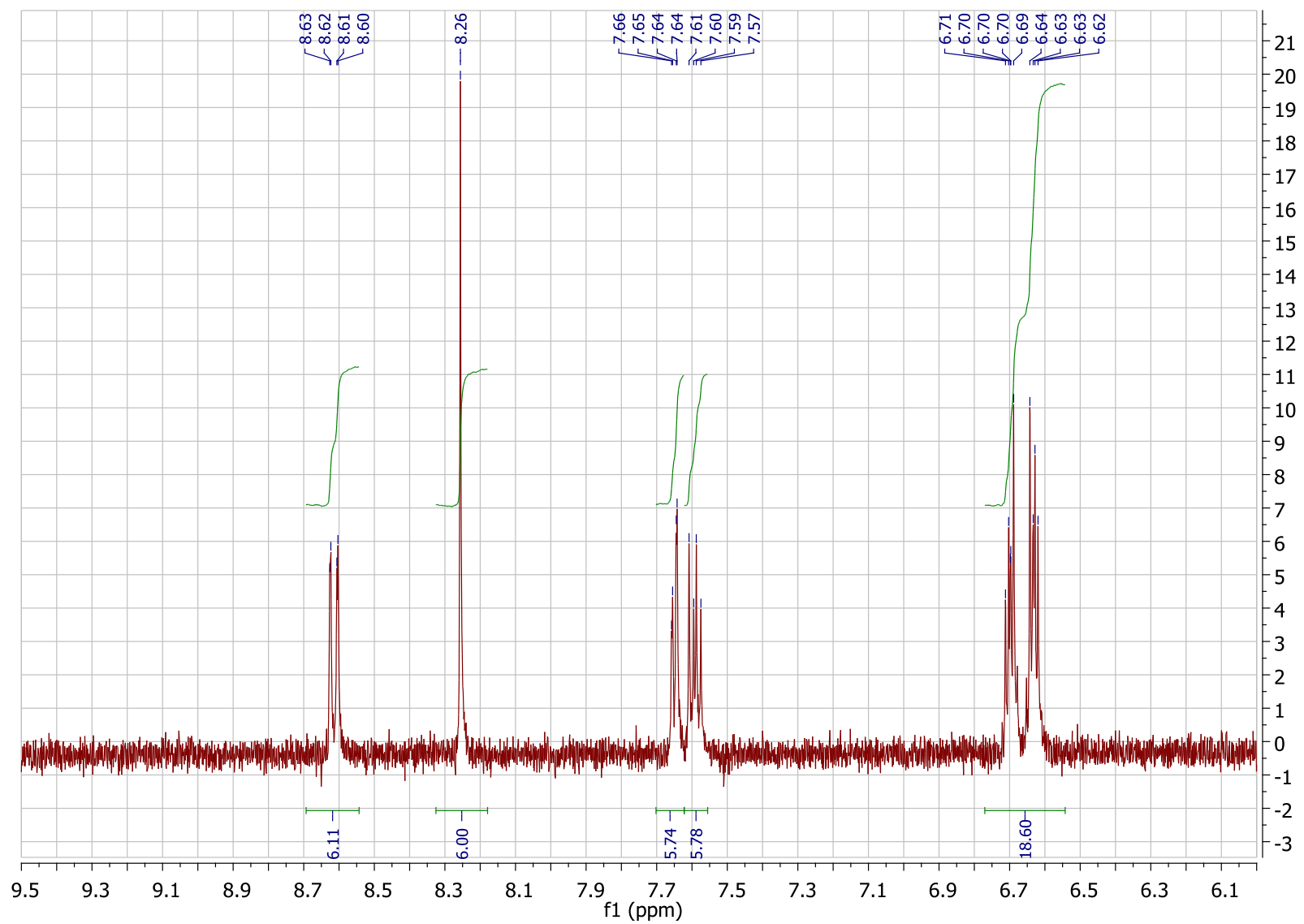


Figure S28c. NMR spectra of [Fe(*phen*)₃](Δ-TRISCAS)₂ (**4**) in d₃-acetonitrile

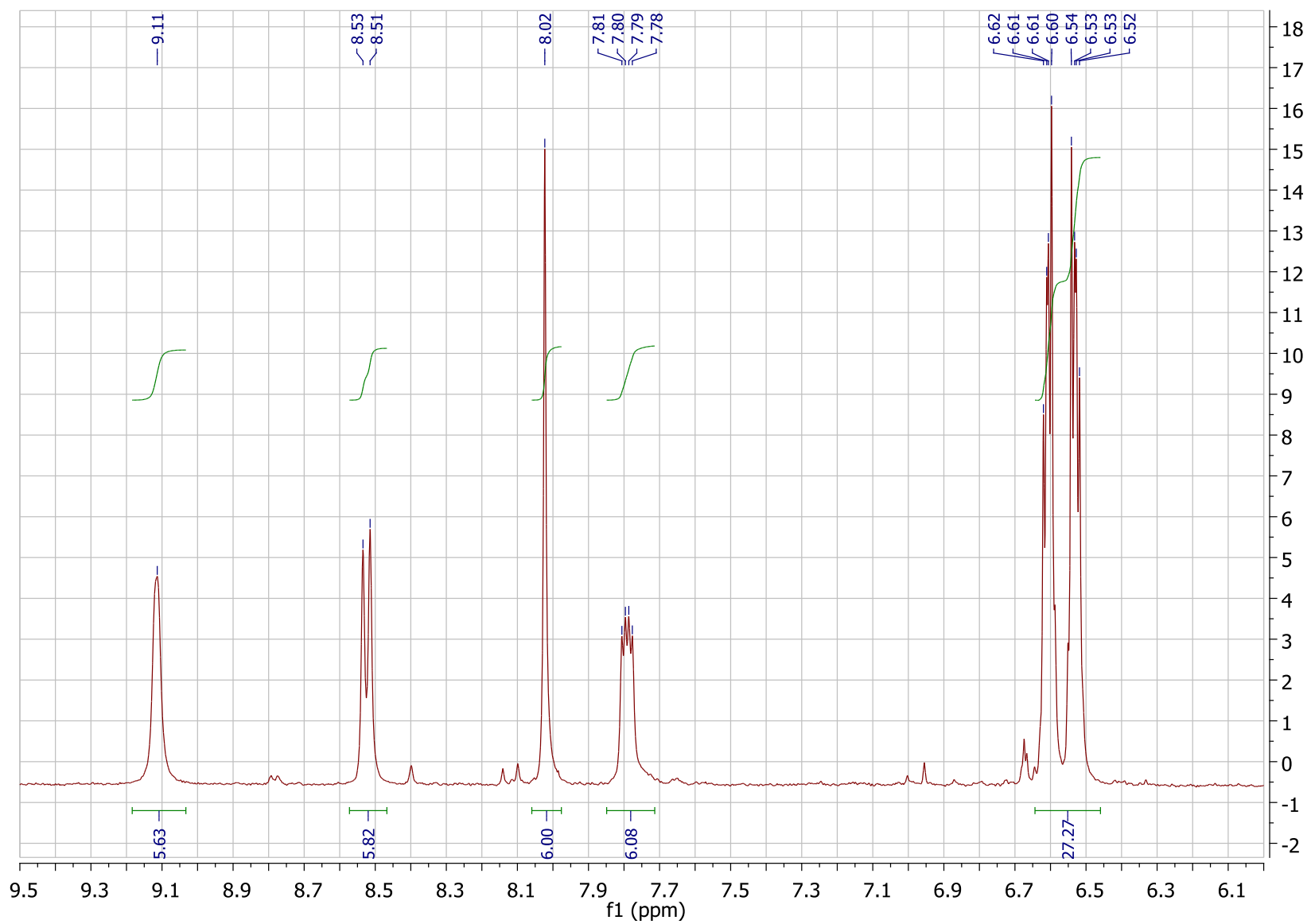
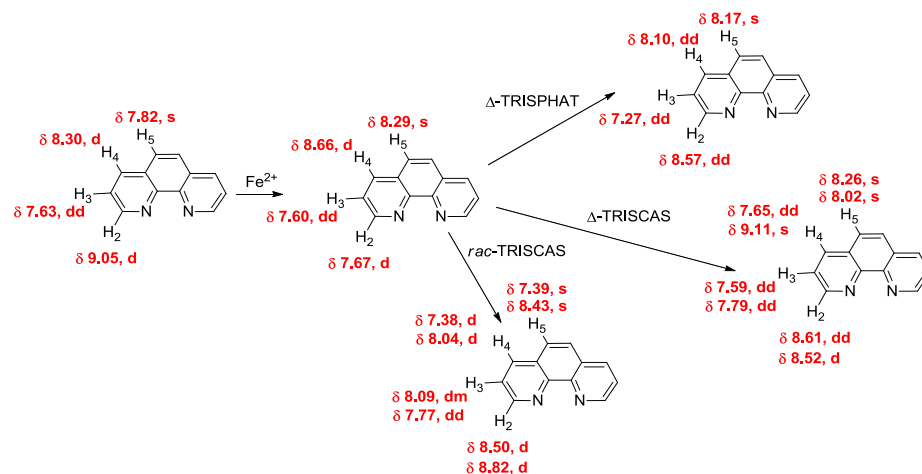


Figure S28d. NMR spectra of [Fe(phen)₃](Δ-TRISCAS)₂ (4) in d₆-acetone

^1H NMR of (**3**) δ (ppm, 400 MHz, CD_3CN) 8.50 (d, $J = 8.1$ Hz, 6H, *phen* H2), 8.09 (dm, $J = 8.2$, 6H, *phen* H3), 7.39 (s, 6H, *phen* H5), 7.38 (d, $J = 2.2$ Hz, 6H, *phen* H4), 6.73 – 6.58 (m, 24H, TRISCAS catechol); δ (ppm, 400 MHz, $(\text{CD}_3)_2\text{CO}$) 8.82 (d, $J = 8.2$ Hz, 6H, *phen* H2), 8.43 (s, 6H, *phen* H5), 8.04 (d, $J = 4.8$ Hz, 6H, *phen* H4), 7.77 (dd, $J = 8.1, 5.2$ Hz, 6H, *phen* H3), 6.60 – 6.44 (m, 24H, TRISCAS catechol).

^1H NMR of (**4**) (d.e.= 88%) δ (ppm, 400 MHz, CD_3CN) 8.61 (dd, $J = 8.1, 1.2$ Hz, 6H, *phen* H2), 8.26 (s, 6H, *phen* H5), 7.65 (dd, $J = 5.2, 1.1$ Hz, 6H, *phen* H4), 7.59 (dd, $J = 8.2, 5.3$ Hz, 6H, *phen* H3), 6.74 – 6.58 (m, 24H, TRISCAS catechol); δ (ppm, 400 MHz, $(\text{CD}_3)_2\text{CO}$) 9.11 (ps, 6H, *phen* H4), 8.52 (d, $J = 8.0$ Hz, 6H, *phen* H2), 8.02 (s, 27H, *phen* H5), 7.79 (dd, $J = 7.8, 4.0$ Hz, 6H, *phen* H3), 6.57 (ddd, $J = 31.5, 5.5, 3.6$ Hz, 24H, TRISCAS catechol).



^1H -NMR shifts in d_3 -MeCN for *phen* and $[\text{Fe}(\text{phen})_3]\text{Cl}_2$ ²⁹, in CDCl_3 for $[\text{Fe}(\text{phen})_3](\Delta\text{-TRISPHAT})_2$ ³⁰, in d_3 -MeCN (upper value) and d_6 -acetone (lower value) for **3** and **4**.

²⁹ L. Pazderski, T. Pawlak, J. Sitkowski, L. Kozerskib, E. Szłyka, *Magn. Reson. Chem.* **2010**, 48, 450.

³⁰ J. J. Jodry, R. Frantz, J. Lacour, *Inorg. Chem.*, **2004**, 43, 3329.

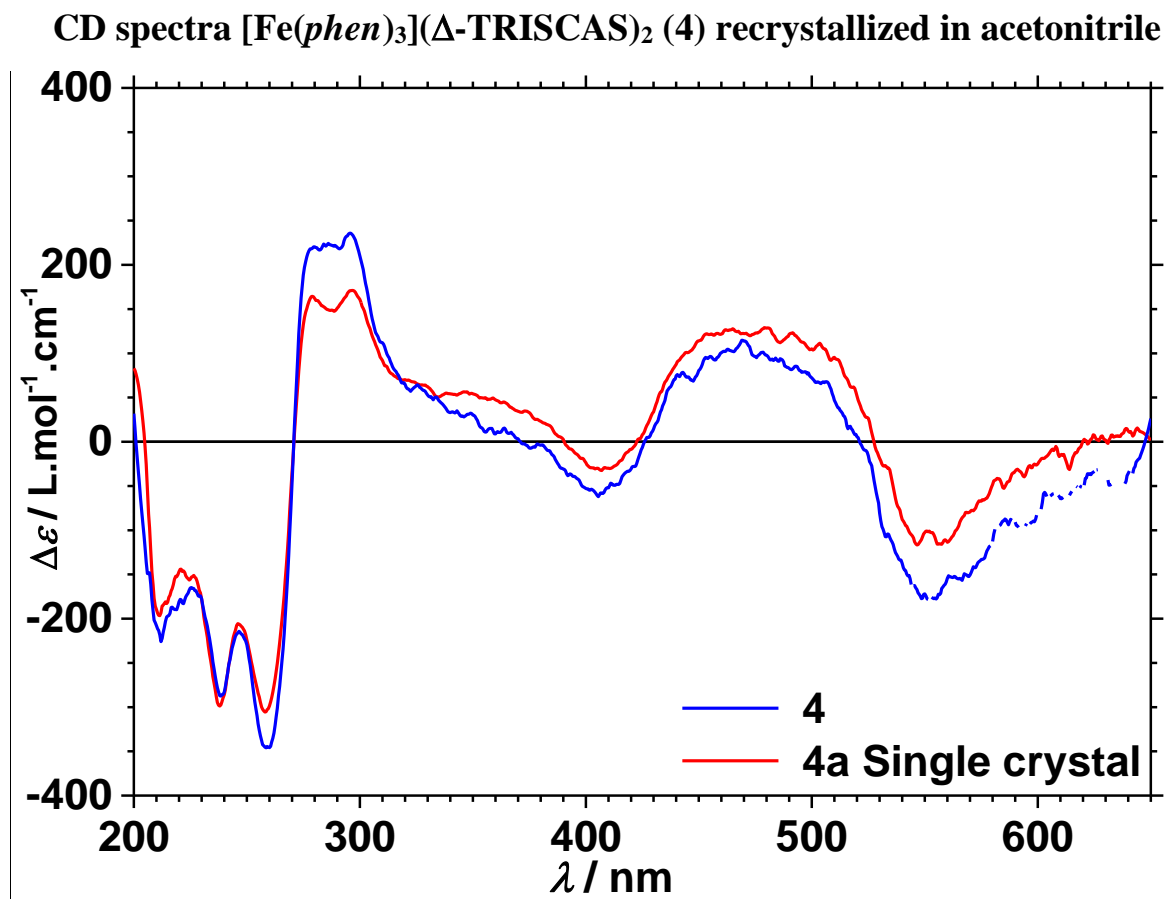


Figure S29. CD spectra of KBr pellets with **4a** recrystallized from acetonitrile.

Single crystal (red line) spectrum compared to a pellet prepared from complex **4** (blue line).

Second-harmonic generation measurements

Drop-cast samples were prepared starting from N,N-dimethylformamide solutions of complexes **4** (8.4 mM) and **5** (7 mM). A drop of 10 μL on a 22 \times 22 mm² glass cover slide was dried in a dessicator connected to a membrane pump. The procedure was repeated three times on the same spot to obtain a satisfactory coverage.

Raman spectrum measurements were performed with a Jobin-Yvon LabRAM HR800 high spectral resolution spectrometer between 0 and 2000 cm^{-1} . A 1200 grooves. cm^{-1} grating was used for the Raman spectral dispersion after excitation with a green Coherent Sapphire 532-50 SF CW solid state laser source (up to 50 mW, $\lambda = 531.97$ nm, TEM 00, single mode). A 100 \times NA 0.9 Olympus objective was used for excitation and visible epi-collected. Laser power was adjusted to avoid damaging the molecular material: laser power was limited to 10 mW, further attenuated by a 10 % filter. The power measured out of the objective was in these conditions about 100 μW . Nevertheless the reduced spot size ($\text{\O}20$ μm) gives fluences above 1 W/cm^2 which were found to be still enough to cause visible damage to the samples with long exposure times.

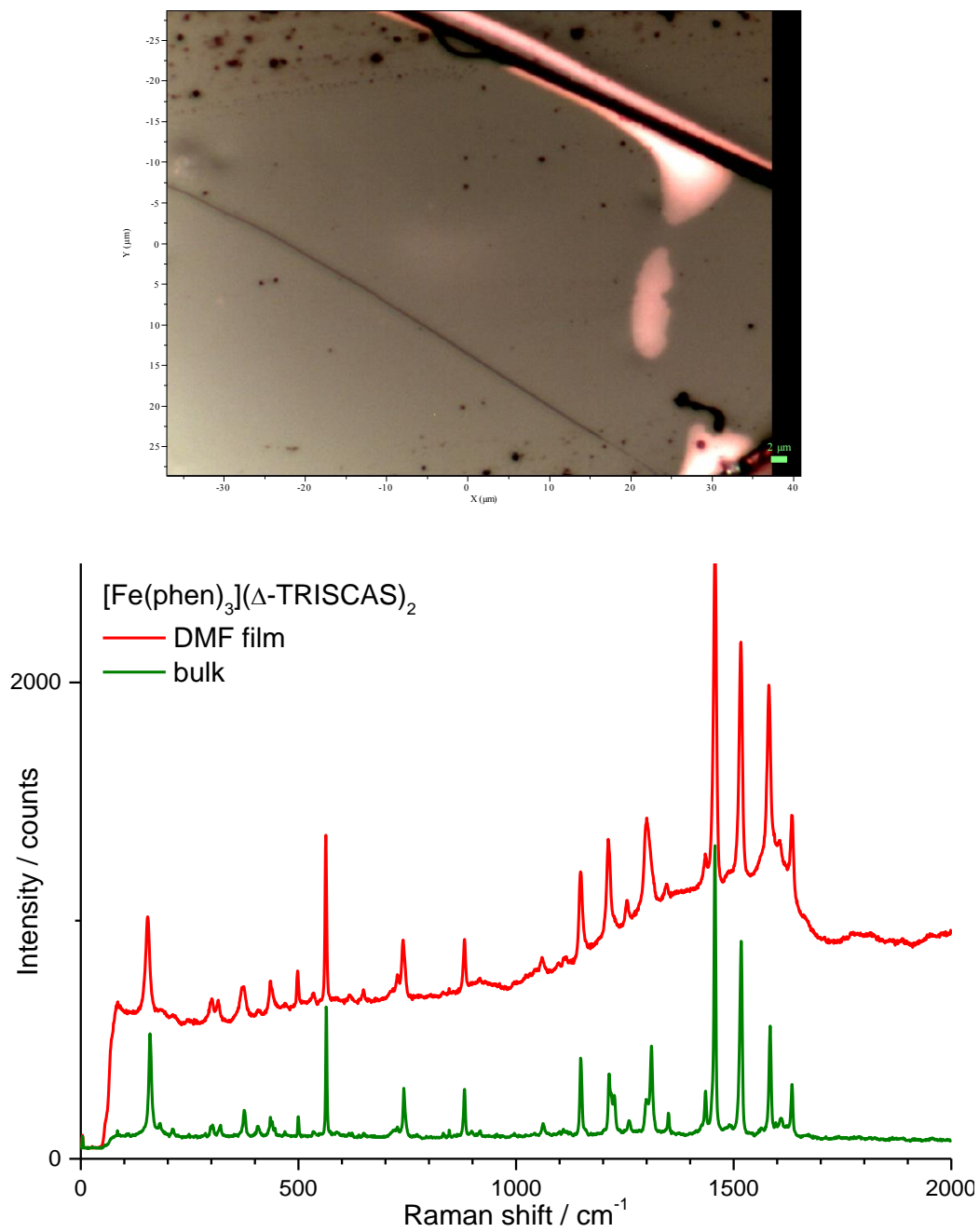


Figure S30. Complex $[\text{Fe}(\text{phen})_3](\Delta\text{-TRISCAS})_2$ (**4**) (top) microscope picture before irradiation of a drop-cast film prepared from a N,N-dimethylformamide solution (bottom) Raman spectrum of the film (red curve) compared to the spectrum measured on a single crystal in the same conditions (green curve).

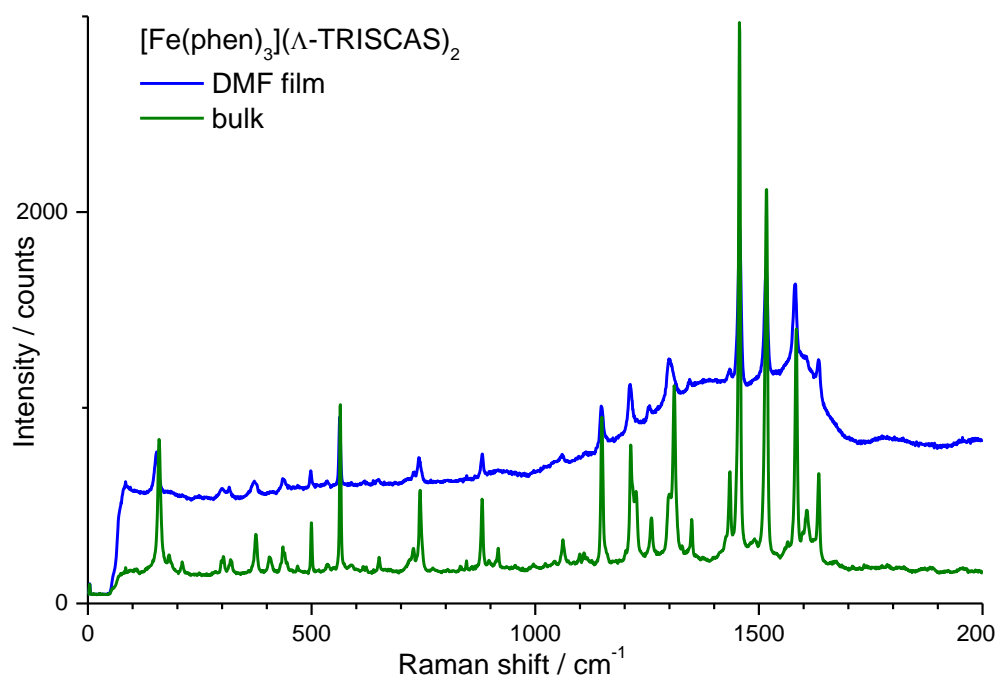
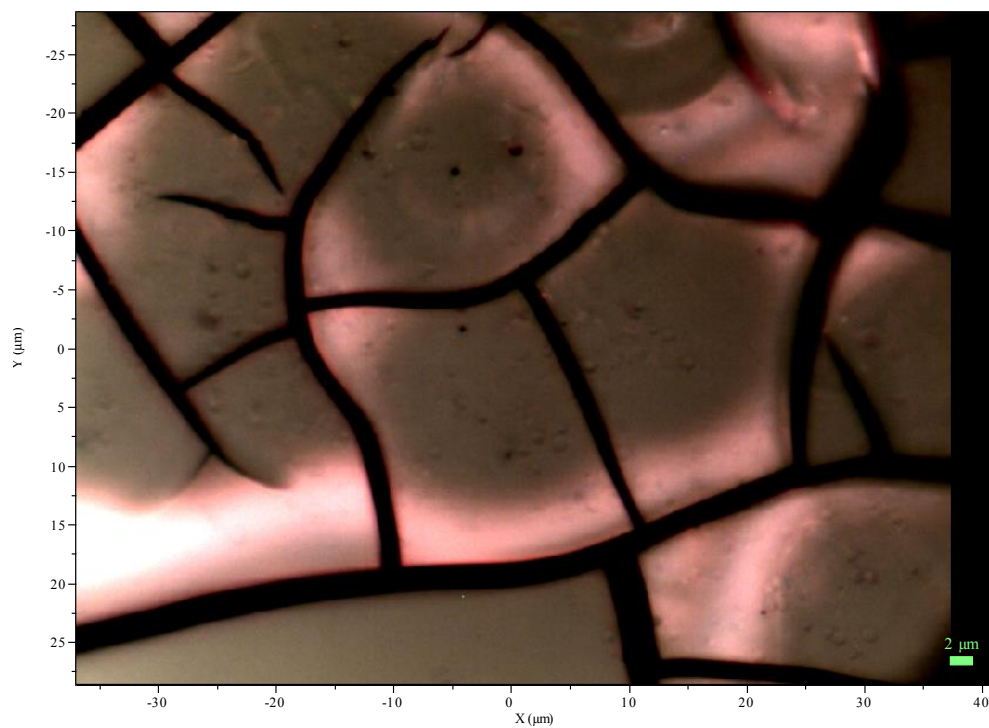


Figure S31. Complex $[\text{Fe}(\text{phen})_3](\Lambda\text{-TRISCAS})_2$ (**5**) (top) microscope picture before irradiation of a drop-cast film prepared from a N,N-dimethylformamide solution (bottom) Raman spectrum of the film (blue curve) compared to the spectrum measured on a single crystal in the same conditions (green curve).

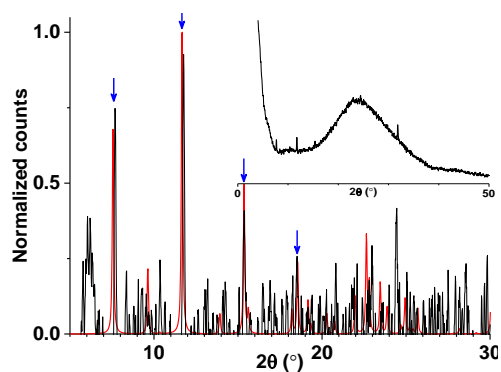
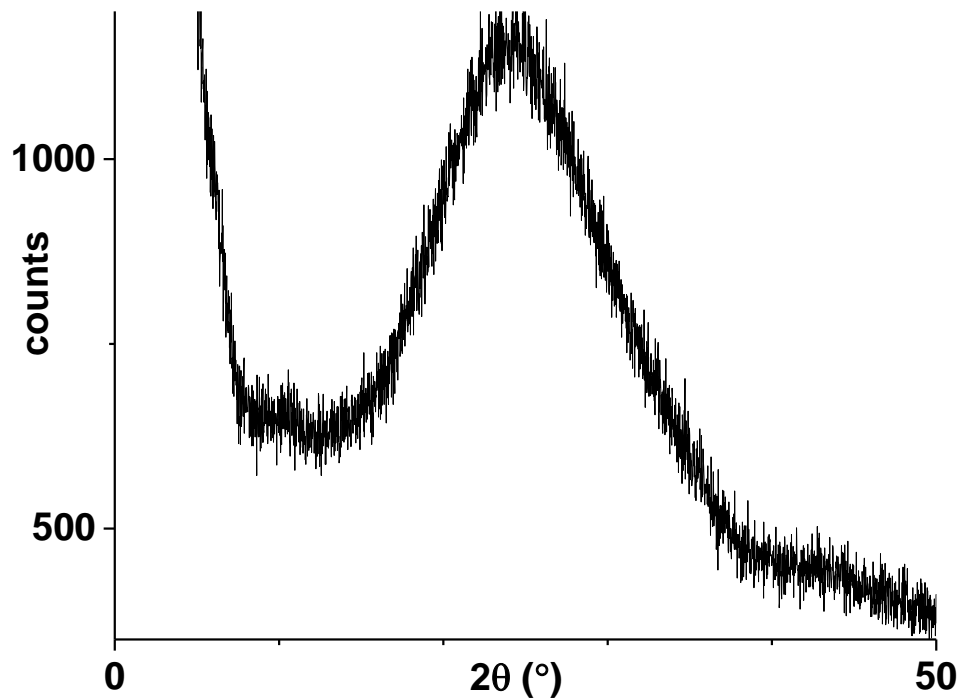


Figure S32. Diffractograms of drop-cast films prepared from N,N-dimethylformamide solutions of complexes $[\text{Fe}(\text{phen})_3](\Delta\text{-TRISCAS})_2$ (**4**) (top) and $[\text{Fe}(\text{phen})_3](\Lambda\text{-TRISCAS})_2$ (**5**) (inset in bottom).

For complex **4** the diffractogram was smoothed and the broad signal due to the amorphous glass substrate was subtracted before comparison with the pattern calculated from the corresponding single-crystal structure (in red). Significant matches are signalled by blue arrows.